Using Fiber-Optic Reflectance Spectroscopy (FORS) to Identify Human Decomposition Fluid Characteristics in Plants Leaves and Soil

A Thesis Presented for the
Master of Arts
Degree
The University of Tennessee, Knoxville

Anielle Duncan
December 2023

ACKNOWLEDGEMENTS

I would like to thank the human body donors of the Forensic Anthropology Center and their families. Without their generous donation this research would not be possible. Thank you to my advisor, Dr. Dawnie Steadman and her years of support, guidance, and mentorship. Thank you to members of my thesis committee, Drs. Amy Mundorff and Sierra Bow who provided support and guidance every step of the way. I would like to thank my colleagues, especially Erin Patrick and Stephanie Goble, and several undergraduate students, who assisted with so many activities at ARF from the beginning to the end of this project. This research, was part of a larger collaboration with the Neal Stewart Plant Genetics Lab and DeBruyn Soil Science Lab, supported by a Defense Advanced Research Projects Agency (DARPA) grant.

ABSTRACT

Anthropologists may be asked by law enforcement or family members to assist in the search for missing deceased individuals. The search areas are often in harsh, rugged terrain for which some technologies, such as ground penetrating radar, cannot be used. Fiber-optic reflectance spectroscopy (FORS) is a portable instrument that can collect information on plants and soil in the surrounding environment, even in austere environments. This study aimed to test whether FORS could be used to identify decomposition fluid in nearby plants and soil in the visible near-infrared (VNIR) and short-wave infrared (SWIR) spectral regions. Using FORS to analyze the spectral signature of human decomposition fluid on the surface soil and in plant leaves can inform whether cadaveric materials are present, and if they persist in the surrounding environment. In forensic contexts, FORS is advantageous due to its portability, non-destructive data collection, and rapid analysis. The goal of this study was twofold; initially, determine whether cadaveric materials provide a spectral signature for human decomposition fluid identifiable in nearby plants and soil, and then to assess if this signature persists. Conducted at the Anthropology Research Facility (ARF) at the University of Tennessee, Knoxville, this study examined a prevalent plant at ARF, amur honeysuckle (*Lonicera maackii*), and soil surrounding n=32 human body donors. The 32 donors were divided into two separate datasets, a longitudinal and cross-sectional dataset. The longitudinal dataset classifies the spectral signature of decomposition fluid and its presence in nearby plants and soil across time during active decomposition. The cross-

sectional data set classifies the spectral signature after cessation of active decomposition, to examine temporal longevity of the spectral signature. The results show that decomposition fluid does have a detectable spectral signature. The signature is identifiable in soil impacted by decomposition fluid. The signature, however, is not present in plant leaves when looking at the selected wavelengths in the VNIR and SWIR regions. The results of this research are significant because it highlights the applicability of using spectroscopic methods to aid in the location of missing deceased individuals through an examination of potentially affected soils.

TABLE OF CONTENTS

LIST OF TABLES

LIST OF FIGURES

CHAPTER ONE

INTRODUCTION

According to the National Missing and Unidentified Persons (NamUs) database more than 600,000 people go missing annually, and approximately 4,400 unidentified remains are recovered each year. Methods for locating missing deceased individuals can be difficult and limited based on technology, terrain, and the available equipment and resources. The effects of decomposition and other taphonomic processes can also complicate the ability to locate missing deceased individuals. Research has found that the environment can directly affect the rate and pattern of human decomposition and vice versa (Carter et al. 2007; Bates and Wescott 2016). It is the interaction between human decomposition and the environment that creates new depositional Characteristics that have the potential to assist in the location of missing deceased individuals.

The purpose of this study was to evaluate whether fiber optic reflectance spectroscopy (FORS), can be used to identify a spectral signature of human decomposition fluid that is taken up by plant leaves and in soil around decomposing human remains. It is theorized that FORS can detect spectral features associated with lipids, carbohydrates, and proteins from human decomposition in plants and soil. FORS provides spectral data readouts as vectors based on the intensity of light representing a different wavelength band (Beattie and Esmonde-White 2021). Janaway et al. (2009) discusses that the human decomposition process results in the release of body fluids containing high concentrations of various lipids, carbohydrates, and proteins. Lipids, carbohydrates, and proteins can be identified at specific wavelengths (Horn 2018). Horn

(2018) used FORS to detect proteins, lipids, and carbohydrates in spectral samples, corresponding to specific wavelength bands in paints that were made from animal and vegetable fats, animal blood, urine, water, and eggs. Therefore, theoretically human decomposition fluid can be detected by FORS.

My research questions address the efficacy of using FORS to identify cadaveric materials from human decomposition in plants and soil:

1. Does human decomposition fluid have a detectable spectral signature that can be found in fluids shed from the body in an outdoor environment?
2. Can human decomposition fluid's spectral signature be detected in plant leaves and soil during active decomposition?
3. Does the spectral signature of human decomposition fluid persist in the plant leaves and soil after the cessation of active decomposition?

To address these research questions, I collected data from two different sample sets, longitudinal and cross-sectional. The longitudinal sample examines the spectral signature throughout the decomposition process, from fresh decomposition through advanced decay. The longitudinal sample was to address the first two research questions to determine if a human decomposition signature is detectable during active decomposition *via* FORS and whether that signature is identifiable in plants and soil during active decomposition. The cross-sectional dataset examines the spectral signature during advanced decay, after the cessation of the release of fluids. The cross-sectional data set is

to determine whether a detectable spectral signature persists after the cessation of active decomposition and can be detected using FORS.

Lipids, carbohydrates, and proteins are released from the body as cadaveric materials in the form of purge fluid on to the soil. These materials are taken up by the plant roots through the soil. The increased presence of lipids, carbohydrates, and proteins from decomposition fluid in both plant leaves and soil should be detectable using FORS. I hypothesize that human decomposition will have a detectable spectral signature that will be identifiable in plants and soil, the signature will be identifiable during active decomposition, and will also persist over time through advanced decay. The signature will be present and persist over time due to the influx of lipids, carbohydrates, proteins, and other compounds introduced from the body to the environment during active decomposition. Results from this study will inform the applicability of using hyperspectral instruments, such as FORS, to locate missing deceased individuals.

This thesis is organized as follows; Chapter Two details remote sensing technologies, including the applicability of FORS. The process of human decomposition and spectral classifications are also detailed in chapter two. Chapter Three discusses the methods and materials used for the research. Chapter Four provides the results addressing each research question. Chapter Five details the interpretations of the results, limitations, and suggests future directions.

CHAPTER TWO

LITERAUTRE REVIEW

Background

Law enforcement often search for missing deceased persons, but technology to assist in such searches can be limited, especially in difficult terrain. Remote sensing technology may have the potential to allow for the detection of decomposing human remains in challenging environments. Brabazon et al. (2020) have proposed that using hyperspectral unmanned aerial vehicles (UVA) to detect a spectral response in the tree canopy may be used to locate a decomposing individual. However, the specific spectral signature for human decomposition fluid must first be characterized. While research has primarily looked at how plants and soil can change spectrally based on different environmental impacts, such as, there has been little research that looks at how human decomposition can be viewed spectrally (Huete et al. 1985, Mandoli et al. 1990, Corcoran 20216, Gürtler et al. 2022). Plants and soil are affected differently as plants uptake and metabolize the decomposition fluid, while the fluid saturates the soil, altering the soil chemistry (Taylor et al. 2023). The soil underneath and the plants around a decomposing body hold information about the cadaver environment. The following subsections will detail the uses of remote sensing and reflectance spectroscopy, the progression and chemical composition of human decomposition, and how stress in plants and changes in soil are visible spectrally.

Remote Sensing

Remote sensing broadly refers to the ability to measure or obtain information from an object at the Earth's surface (Aggarwal 2004, Gupta 2018). Remotely sensed information is obtained by a 'remote' recording device, meaning it does not come into direct contact with the object being analyzed. Some remote sensing devices collect data in the form of spectra (Aggarwal 2004, Gupta 2018). Spectral data is defined as plotted information on the electromagnetic spectrum (EMS) that is the function of either a wavelength or the frequency of light (Gupta 2018). Spectral signatures are identified by their function of wavelength as either absorption or reflectance (Brown et al. 2006). The basic principle of remote sensing through spectral analysis is that various wavelength regions of the electromagnetic wavelength spectrum reflect at various intensities depending upon the physical and compositional makeup of the object (Gupta 2018).

Types of remote sensing technology include light detection and ranging (LiDAR), thermal imaging, and spectroradiometers, such as FORS. LiDAR is a type of radar imaging remote sensing technology that uses lasers to provide a detailed representation of terrain topography (Campbell and Wynne 2011). LiDAR has recently been used in forensic contexts to track changes in the surface elevation of burials (Corcoran 2016; Corcoran et al. 2018). Thermal imaging measures an object's infrared energy and converts that to temperature, which can be viewed in the far infrared regions of the EMS (Campbell and Wynne 2011). Thermal imaging can detect the thermal properties and surface temperatures of materials such as soil, rocks, vegetation, and other objects on or

under the Earth's surface (Campbell and Wynne 2011). In a forensic context, thermal imaging has been used to determine the thermal signature changes of decomposition for remote detection via drone (Butters et al. 2021).

Spectroscopy instruments, such as spectroradiometers and hyperspectral drones, can be used remotely to separate and measure spectral data (Campbell and Wynne 2011; Merwe et al. 2020). Spectroradiometers that record data in the ultraviolet, visible, and near-infrared (UV-VIS-NIR) spectroscopy have been used in soil science to interpret soil characteristics (Aitkenhead-Peterson et al. 2020, Campbell and Wynne 2011). Spectroradiometers produce a spectral response curve with a wavelength range of 300-2500 nm. These bands include the EMS's visible, near-infrared (NIR), and short-wave infrared (SWIR) wavelength regions. Spectral response curves show the intensity of radiation emitted or reflected by objects (Gupta 2018). Aitkenhead-Peterson et al. (2021) have used spectroscopy to investigate the use of ultraviolet, visible, and UV-Vis-NIR wavelength ranges to determine if soil spectra can be used to estimate the PMI of an individual using a Lab-Spec 5000. This study did not examine plants but found that there is the potential to us soil analysis for estimating PMI.

Hyperspectral unmanned aerial vehicles (UVA), also known as drones, have been used in agriculture and plant ecology sciences to monitor information such as plant health, crop damage, plant height and size, and soil conditions (Merwe et al. 2020, Sun et al. 2021). Individual plant species can be classified spectrally using hyperspectral UAV while determining the spatial relationship to other plants (Sun et al. 2021). UAV can

classify the morphology and physiological status of plants. Sun et al. (2021) discuss that UAV can be used to conduct forest phenology studies that identify plants' biochemical and physiognomic characteristics. The hyperspectral analysis from spectral data collected by UVA can identify certain macronutrients in the spectra, such as nitrogen, carbon, and magnesium (Capelle and Macko 2016).

Remote sensing devices are classified as either active or passive. Active remote sensing refers to when energy is provided by the particular instrument (Campbell and Wynne 2011). The sensors in active devices have built-in light source that is used to collect data (Campbell and Wynne 2011). Passive remote sensing refers to technology that uses an external energy source, such as the sun, and these sensors use external energy to collect data. (Aggarwal 2004; Campbell and Wynne 2011). The ASD FieldSpec 4 Standard-Res Spectroradiometer, used in this research, contains an active sensor.

Fiber-Optic Reflectance Spectroscopy

While traditional remote sensing instruments like LiDAR sense from a considerable distance, other instruments can be used more near and come into contact with the object under analysis. An example of this is a spectroradiometer, such as the ASD FieldSpec 4 Standard-Res Spectroradiometer. Spectroradiometers produce a spectral response curve on the EMS depending on the instrument’s detectors and capabilities (Gupta 2018). Spectral information is measured based on electromagnetic energy by either reflecting the material at the surface of an object. Reflectance spectroscopy is a function of a wavelength based on differential reflection and light

scattering (Bow 2020). Reflectance spectroscopy can also be defined as the ratio of irradiance, or light coming off an object, to the incident light, or that light that illuminates a surface (Bow 2020). At the same time, spectral reflectance can be described as the percentage of light reflected from a particular object (Gupta 2018). Important definitions of the process of reflectance spectroscopy include reflectance and reflection. Reflectance is the relative brightness of a surface based on the specific wavelength interval for the object being measured, while reflection occurs when a ray of light is redirected as it hits a non-transparent surface. Specular reflection occurs when incident radiation is redirected in one direction for materials of a smooth surface (Campbell and Wynne 2016). Many disciplines, such as geology, agriculture, forestry, and hydrogeology, use spectroscopy to characterize a variety of surfaces (Gupta 2018).

Spectral signatures are created from the electronic transition of atoms and vibrational bending and stretching of structural atoms that form molecules (Brown et al. 2006). FORS, a type of reflectance spectroscopy, uses a fiber-optic cables to cast an incident beam into a sample. The incident beam is then reflected to the sensor and collected by the fiber optic cables (Bow 2020). When collecting data, spectral software depicts the data collected by the fiber optics of the sensor as a waveform on the EMS that displays reflectance values as peaks on the spectrum and absorption features as valleys, which can be broad or narrow depending on the sample being collected (Bow 2020).

Field spectrometers collect spectra at various parts of the EMS, but they all have two main components, an optical system, and a detector system (Gupta 2018). The

optical system collects radiation between the light source and the object under analysis. The optical system then converts that radiation into an electromagnetic signal on the wavelength spectrum (Gupta 2018). The detector converts the radiation intensity into the electrical signal that provides the spectra (Gupta 2018). Spectral data can be viewed on the EMS in ranges of 300-1000 nm, which includes visible light and near-infrared regions (VNIR), and 1000-3000 nm, which provides the short-wave infrared regions (SWIR) of the EMS (Gupta 2018; Bow 2020) (Figure 2.1). Key spectral features for different compounds peak differently on the wavelength associated with certain spectral bands. The peaks are based on the reflection and absorption values emitted from the object (Gupta 2018). The different spectral values associated with bands allow for differentiation between types of objects under analysis. For example, healthy versus dry plants will have different reflectance values based on their molecular compositions, such as chlorophyll levels, magnesium, and water content (Figure 2.2).

Spectral response curves indicate the intensity of reflected light from an object, this is also referred to as a spectral signature (Gupta 2018). When viewing spectral data in relation to the EMS, an increase in visible light at the time a sample was taken results in a decrease in near-infrared reflectance on the data output (Chaerle and Van Der Straeten 2000). When collecting spectral data on plants and soil in the field it is important to control for light interference and atmospheric water bands. To control for light and and atmospheric water bands, using an internal light source, such as a contract probe that accompanies an instrument is necessary (Milton et al. 2009). The light source from a

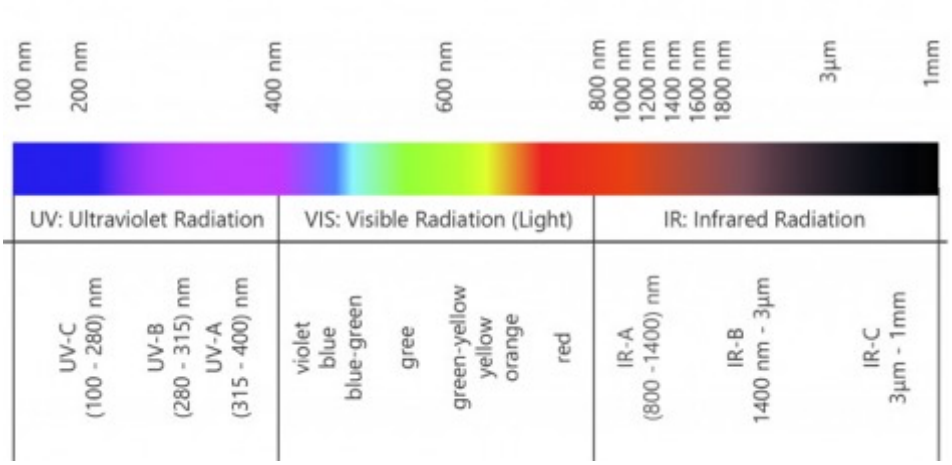

Figure 2.1: Electromagnetic Spectrum (https://www.gigahertz-optik.com/en-us/service-and-support/knowledge-base/basics-light-measurement/light-color/opt-rad-wavelength-range/)

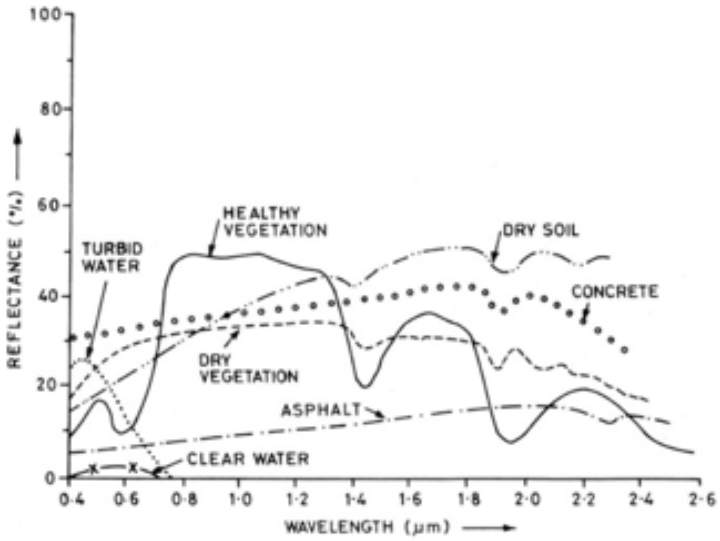

Figure 2.2: Different reflectance and absorption features for various spectral materials (Gupta 2018: 33)

contact probe provides standardized illumination of the object so that subtle absorption features can be seen in SWIR regions (Milton et al 2009). Controlling for light by using a contact probe allows for reproducible measurements of objects and reduces uncertainty of what is actually being collected (Milton et al 2009). The presence of lipids, carbohydrates, and proteins in a spectral response of human decomposition fluid has not yet been examined; however, to characterize the spectra of decomposition fluid, it is necessary to understand the processes of human decomposition and how it affects the surrounding environment.

Human Decomposition

Decomposition is a natural process that alters biological and chemical characteristics of the surrounding environment (Carter et al. 2007). Because of this alteration to the environment, plants and soils are becoming an increasingly important area of interest within decomposition research (Corcoran 2016; Brabazon et al. 2020, Taylor et al. 2023). Studies have shown that specific soil components can be used as a mechanism to determine a postmortem interval (PMI) (Carter and Tibbett 2008; Forbes et al. 2017). Human decomposition occurs as a progression and can be divided into stages, such as autolysis, putrefaction, advanced decay, and skeletonization (Marks et al. 2009). The focus for this thesis is on putrefaction and advanced decay stages, as this is when decomposition has the most significant impact on the direct environment. The decomposition rate is influenced by intrinsic and extrinsic factors, such as temperature,

environment, season, and body composition (Carter and Tibbett 2008; Mason et al. 2022).

Autolysis or the fresh stage of decomposition, is cell breakdown by intrinsic enzymes (Janaway et al. 2009). During autolysis, there are no macroscopic changes visible on the body. Putrefactive changes occur as a result of the increased growth of anaerobic bacteria found in the gastrointestinal tract. The growth and activity of these enteric bacteria cause the first visible changes at the macroscopic level, including green discoloration in the abdomen from the formation of sulph-haemoglobin that later extends through to the chest, arms, and thighs results in marbling. Marbling appears as a red/greenish-red color. The body will continue to discolor due to more sulph-haemoglobin settling in the blood (Janaway et al. 2009). Hydrogen sulfide, carbon dioxide, methane, ammonia, sulfur dioxide, and hydrogen gases are generated through autolysis (Janaway et al. 2009). These gases result from autolysis and bacterial lysis, or breakdown. Volatile fatty acids are also present from anaerobic fermentation.

During putrefaction, by-products of the anaerobic respiration of bacteria create gases that cause bloating in the abdominal cavity (Dautartas 2018). As the body goes through putrefaction, gases, microbes, and liquid by-products are released from the body (Hyde et al. 2017). Pressure from the gases inflate the abdomen, which forces the release of fluid from the body orifices, also known as purge (Dautartas 2018). After the purging of gases and fluid from the body followed by the cessation of bloating, active decomposition begins (Vass 2001; Dautartas 2018).

During active decomposition, protein decay, or proteolysis is driven by enzymes and is influenced by moisture, bacteria, and temperature. Proteolysis creates peptones, polypeptides, amino acids, and gases such as carbon dioxide, ammonia, and methane. Lipids are broken down by hydrolysis and results in the formation of fatty acids (Janaway et al 2009). Carbohydrates are broken down and oxidized to create carbon dioxide and water (Forbes 2008; Janaway et al. 2009). Skin disintegrates, along with other soft tissues, and as this occurs the remaining internal tissues are exposed to the environment, increasing anaerobic bacteria, and accelerating decomposition (Dautartas 2018). As body fluids continue to shed, bones may be exposed, and the remains will begin drying out. Mummification may also occur (Dautartas 2018). Ultimately, skeletonization will occur if not mummified. Skeletonization occurs when bloating has completely subsided, and soft tissues continue to disintegrate (Marks et al. 2009). Skeletal decomposition occurs when all soft tissue is consumed, and the skeleton is completely disarticulated (Marks et al. 2009). Other taphonomic events can occur during skeletal decomposition, such as scavenging and weathering of bone (Marks et al. 2009).

Some of the factors that affect decomposition include temperature, moisture, insect activity, and animal scavengers. The ambient temperature affects the rate of decomposition because both the internal and external microbial processes are affected by the temperature with 15°C and 35°C promoting peak bacterial activity (Janaway et al. 2009; Dautartas 2018). Putrefaction occurs optimally between 21°C and 38°C and is slowed at temperatures below 10°C or above 40°C (Forbes 2008). Insect activity is also

highly dependent on temperature. Insect colonization can occur within hours of death, as gravid female flies are attracted to oviposit eggs onto the remains (Janaway et al. 2009). As the eggs hatch, the larvae begin to consume the body by liquifying the tissues, which reduces body mass and produces the decomposition fluid that saturates the soil. Scavengers can also affect the rate of decomposition, as canids and rodents often consume and disarticulate the body during the process of decomposition (Dautartas 2018). Other factors that can impact decomposition rates include microorganisms found in the soil, the overall soil chemistry, and fungi (Carter and Tibbett 2008). Changes to soil and plants as a result of decomposition can be found in the cadaver decomposition island (CDI).

Cadaver Decomposition Island (CDI) and Plant and Soil Nutrient Metabolomics

The interaction between a decomposing body and the soil results in changes to the environment (Cobaugh 2013; Barton et al. 2020). During putrefaction and active decay, the release of decomposition fluid enters the soil and surrounding environment, and a CDI is formed. A CDI is the spatially defined area where decomposition fluid extends outside of the body during putrefaction. The dynamic interaction between decomposition fluid and soil within the CDI has recently become an essential forensic resource (Cater et al. 2007; Carter and Tibbett 2008; Taylor et al 2023). The amount of decomposition fluid released and, hence, the size of the CDI increases with insect and microbial activity. Decomposition fluid releases carbon, nitrogen, ammonium, nitrate phosphorus, calcium, potassium, sulfate, magnesium, chloride, sodium, manganese, and other base cations in

the soil as well as proteins, nitrates, carbohydrates, and lipids (Cater et al. 2007; Carter and Tibbett 2008). Once these elements are released into the soil, the surrounding environment (e.g., plants and microbes) take them up in their nutrient cycles (Forbes et al. 2017).

The biophysiochemical makeup of a CDI changes over time and is defined by the succession of insects, plant, and fungal communities (Cobaugh 2013). The concentration of chemical compounds, such as ammonium and nitrate, also changes over time (Carter and Tibbett 2008). Decomposition fluid impacts the soil by lowering the pH levels, increasing the amount of nitrogen, ammonium, and calcium present, and lowering the amounts of sulfates and carbon in the soil (Aitkenhead-Peterson et al. 2012, Taylor et al. 2023). The lateral boundaries of a CDI have been found to extend about 2.2 meters away from the body. The vertical depth of the CDI does not appear to penetrate below the surface. Cobaugh et al. (2015) sampled soil zero to three centimeters below the surface and did not find significant changes to the soil pH below the surface. However, the boundary changes over time depending on the size of the body, the size and extent of maggot masses, and the type and texture of the soil (Cater et al. 2007; Carter and Tibbett 2008). The size of the CDI expands during active decay. The soil and plants located within the CDI will be altered due to the chemical process of decomposition (Forbes et al 2017).

The chemicals released from the body that form the CDI directly affect the ability

of soil and plants to metabolize nutrients. These nutrients include nitrogen in the form of amino acids, lipids, and carbohydrates. Nitrogen stays in the soil for one to four years after decomposition, meaning that the CDI maintains a presence in the environment well after decomposition ceases (Cater et al. 2007; Carter and Tibbett 2008). This could mean that plant communities surrounding a decomposing body may also be affected for years after decomposition (Hyde et al. 2017). Plant communities are affected by the soil chemistry and microbial communities as well. The interaction between plants and soil occurs in the rhizosphere (plant roots) (Brabazon et al 2020; Hyde et al. 2017). As the soil maintains cadaveric chemicals, these materials are being taken up in the rhizosphere, causing plant stress (Brabazon et al. 2020). Plant stress can be attributed to the influx of decomposition fluid because it impacts the pH of the soil. Decomposition fluid released into the soil causes the soil to become acidic and the soil remains acidic even after active decomposition (Taylor et al. 2023).

Plants are directly taking up their nutrients from the soil; therefore, the condition of the soil plays a critical role in the plant's biology (Karamanos 2013). Plants will metabolize nutrients from the soil through chemical processes that will break down or synthesize the nutrients depending on the type and conditions. Whether a plant takes up nutrients is influenced by the species, environmental conditions, and the interaction between plants and soil (Karamanos 2013). Plants uptake nutrients through three mechanisms: mass flow, diffusion, and root interception. Mass flow occurs when nutrients located in water are taken up by the roots. Nitrogen is typically metabolized by

mass flow. Diffusion is when nutrients of high concentration in the soil at the root's surface are transported to areas with no nutrients (Karamanos 2013). Root interception occurs when the roots of the plants come into contact with the nutrients (Karamanos 2013). Given the nature of decomposition fluid, each of these metabolization processes can be attributed to its uptake in plants. In addition to nitrogen, lipids are also taken up by plants and are essential for the plant's cell health. Lipids in plants are responsible for regulating their metabolism (Kim 2020). Carbohydrates, also taken up by plants, provide energy to plants through photosynthesis and regulate both abiotic and biotic stressors to the plant. Increasing the amount of carbohydrates, a plant consumes can provide immunity to plants fighting pathogens, ultimately enhancing plant health (Trouvelot et al. 2014). This may cause the plant to grow back healthier after being affected by decomposition fluid.

Soil pH changes directly affects plant health (Alam et al. 1999). Low pH in soil can affect the growth rate of plants and the possible absorption of minerals. Plant roots are directly affected by the soil pH; this in turn, affects the plant's ability to metabolize nutrients and grow (Alam et al. 1999). Given these biological processes of plant nutrient metabolomics and their relatedness to soil pH, the influx of decomposition fluid in the soil can affect how a plant uptakes nutrients. Plants impacted by decomposition fluid will initially die. However, the plants will regrow, sometimes healthier than before, particularly for colonizing or opportunistic plants due to the increased available nutrients deposited by the cadaveric materials in the soil (Forbes et al. 2017). The increase in

available nutrients released from the body are in the form of lipids, carbohydrates, and proteins. The question remains; since plants often regrow healthier than before and decomposition fluid materials stay in the soil even after active decomposition, will any residual decomposition fluid taken up by plants result in detectable spectral changes of the presence lipids, carbohydrates, proteins in the NIR-SWIR wavelength regions?

Spectral Classifications

Objects are spectrally classified based on where their absorption and reflectance values are located along the EMS. The classification depends upon the sampled material's structural, chemical, and physical properties. The changes to plants and soil chemistry due to decomposition fluid may not be visible to the human eye, but these changes are identifiable spectrally (Corcoran 2016). Spectral analysis on soils and plants is a mechanism for understanding how various stressors affect them. Corcoran (2016) found that vegetation spectra associated with human burials can be separated from spectra from vegetation in undisturbed soil. Spectral differences from vegetation over human burials differ between spring and autumn seasons (Corcoran 2016). Corcoran (2016) analyzed wavelengths of targeted plants at 707-708 nm in the autumn and 761 nm in the spring, as well as 2000-2200 nm corresponding with nitrogen and chlorophyll reflectance. There is a correlation between increased nitrogen in the soil and the chlorophyll production of targeted plants over the burials. The interaction of human decomposition fluid with the

environment can be visible in the reflectance at certain wavelength values of plants and soil. Important wavelength bands for analyzing the spectra of plants, soil, and cadaveric materials are discussed below.

Reflectance Spectroscopy of Plants

Reflectance spectroscopy has been used to detect plant stress in multiple contexts and provides information about how plants use nutrients, light, water (Schweiger 2020). Reflectance spectroscopy has also been used to estimate nitrogen levels in plants (Capelle and Macko 2016, Corcoran 2016, Muñoz-Huerta et al. 2018). Spectral appearances of plants depend on chemical, structural, anatomical, and morphological leaf compositions (Schweiger 2020). The plant height, shape, canopy structure, and foliage are characteristics that affect the appearance of plant spectra (Schweiger 2020). The spectrum of a healthy green leaf absorbs light in the visible spectral regions with a peak at 550 nm (Gupta 2018). The carotenoid pigments associated with chlorophyll are found at 480 nm. At 680 nm, there also is an absorption feature corresponding to the magnesium component of chlorophyll. A near-infrared (NIR) plateau begins at 800 nm to 1300 nm, corresponding to leaf tissue and its cellular structure (Gupta 2018). The rise in reflectance at 800 nm is due to the red edge of chlorophyll absorption bands (Figure 2.3) (Gupta 2018). While these are characteristics of a healthy plant, stressed plants will have decreased reflectance in the NIR regions, and the red band absorption feature will be short and shallow (Gupta 2018) (Figure 2.3).

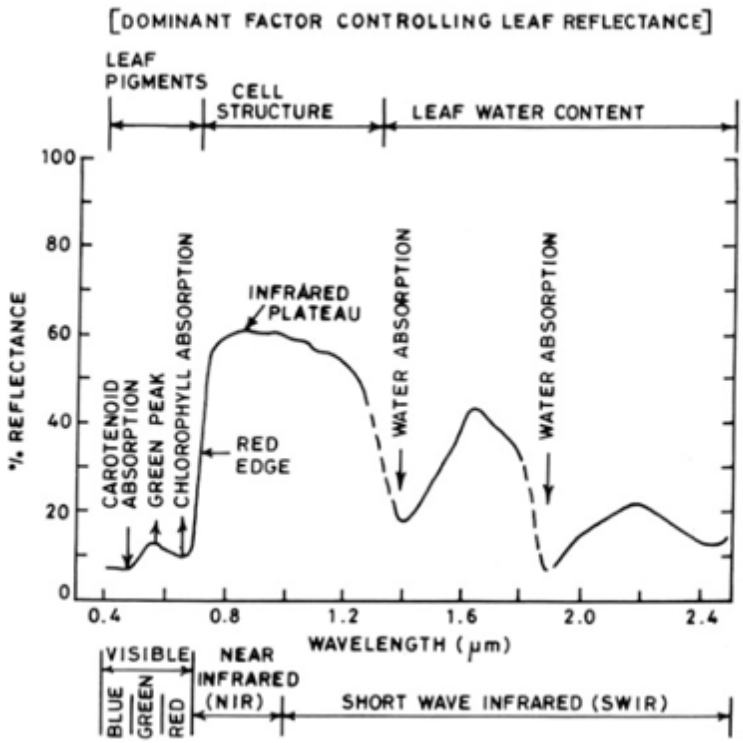

Figure 2.3: Reflectance output of green vegetation in the VIS-NIR-SWIR regions (Gupta 2018:34).

Plants become stressed when they are unable to adjust between a disruption in their physiological homeostasis due to environmental factors (Jansen and Potters 2017). Plant stress is any disturbance that affects the growth and health of the plant and can be defined as either abiotic or biotic (Jackson 1986). Abiotic plant stress can be characterized by environmental conditions, such as temperature, light, and chemicals, that reduce growth while biotic stress includes insects and infectious disease (Cramer et al. 2011; Gull et al. 2019). Abiotic stress causes both physiological and anatomical changes to occur in the plant (Jackson 1986). Leaf color may change as a result of water deficiency, plant pathogens, or chemical changes within the plant (Jackson 1986). Plant stress can also be defined as a temporary, non-optimal state of being before that plant either dies or reaches an equilibrium (Jansen and Potters 2017). The health of plants can be seen by the human eye when the leaves exhibit conditions such as curling or drooping; however, spectroscopy allows for the detection of plant stress before visible changes can be seen (Jackson 1986).

FORS uses the VIS-NIR region is used to detect plant stress (Jones and Schofield 2008). The overall reflectance value depends on the health and condition of the chlorophyll in the leaves (Jones and Schofield 2008). Carbon, hydrogen, oxygen, and nitrogen are essential elements in plants that regulate chlorophyll production (Muñoz-Huerta et al. 2013). As part of various enzymatic proteins of the plant, nitrogen is also responsible for regulating plant growth (Muñoz-Huerta et al. 2013). Plants absorb nitrogen through the soil. Nitrogen taken up by plants may be altered by ammonium and

nitrate which are by-products of decomposition fluid (Muñoz-Huerta et al. 2013). Because nitrogen is an enzymatic protein, the excess nitrogen taken up by the plant may be visible in the NIR-SWIR regions of the spectra. Plant stress is often shown in the color of the plant due to the lack of chlorophyll and this can be seen spectrally within 400 nm-750 nm of the VNIR (Jones and Schofield 2008). A nitrogen deficiency leads to a yellowing of plants due to lack of chlorophyll.

Reflectance Spectroscopy of Soil

Reflectance spectroscopy of soil is a rapid mechanism for soil analysis (Reeves 2010). Spectral features that indicate the presence of soil material are found in the 700-2500 nm range, with most information in the mid-infrared ranges (Brown et al 2006). Soil reflectance found in the VNIR region includes organic material, minerals, salt, and poorly-crystalline andic (containing weathered volcanic glass or pumice) materials (Brown et al 2006). Moisture, organic carbon, and total nitrogen present in the soil can be determined by viewing the VNIR regions of the EMS (Nduwamungu et al 2009). Reflectance values change when more moisture is present in the sample (Figure 2.4). NIR reflectance spectroscopy can provide information about soil compositions in both the topsoil and subsoil (Dunn et al. 2002). In topsoil there is high accuracy in providing spectral information regarding the concentrations of calcium, magnesium, soil pH, and organic soil carbon. In the subsoil there is high accuracy in providing spectral information about the concentrations of sodium, calcium, magnesium, and soil pH (Dunn et al. 2002).

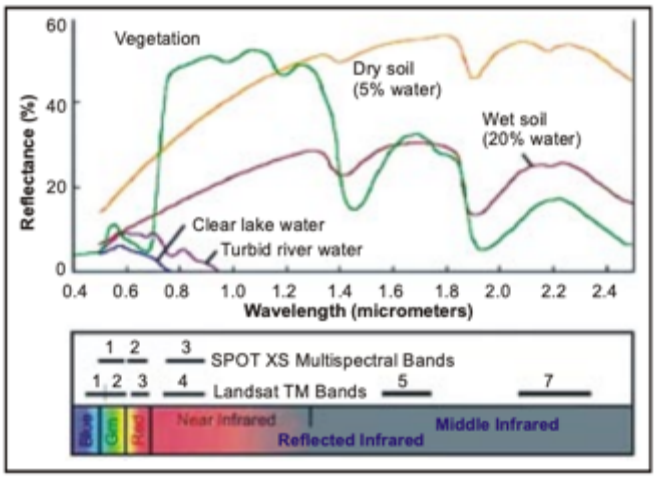

Figure 5. Typical Spectral Reflectance curves for vegetation, soil and water

Figure 2.4. Image indicating the differences in reflectance values for wet versus dry soil (Aggarwal 2004:33).

Reflectance values that determine the moisture content, organic soil carbon, and total nitrogen in soil can be found at 1702-2052 nm (Summers et al. 2011). Depending on the concentrations of moisture content, organic soil carbon, and total nitrogen materials the absorption features the spectra will fluctuate (Summers et al. 2011). The presence of soil carbonate and its absorption features can shift across the EMS depending on what impurities are present in the soil sample. The amount of the sample present, along with the particle size and porosity of the soil sample will determine its absorption features (Summers et al 2011). Clay features can be found at 2200 nm, carbonate features can be found at 2300 nm, and moisture content can be found at 1400 nm and 1900 nm (Summers et al. 2011). The features at 1400 nm and 1900 nm are also known as water bands. When increasing the clay content of soil, a more pronounced absorption feature is present at 2200 nm (Summer et al 2011). Reflectance spectroscopy can also be a tool to evaluate soil contaminates such as heavy metals, organic chemicals, and excess sulfur (Schwartz et al 2011). Plant stress can also be used as an indicator of soil contamination that is visible in the VNIR-SWIR regions (Schwartz et al 2011). Human decomposition fluid is a type of soil contaminate as it alters the nitrogen, carbon, and pH levels (Mason et al 2022, Taylor et al 2023). Because soil contaminates are able to be identified in the VNIR-SWIR regions, it is expected that human decomposition fluid will be detected spectrally in soil.

Spectral Classification of Cadaveric Materials

Lipids, carbohydrates, and proteins also have spectral signatures visible on the EMS and are likely key to detecting decomposition fluid. Using an ASD FieldSpec 3, Horn (2018) identified spectral signatures of lipids, carbohydrates, and proteins in paint made with animal and vegetable fats, animal blood, urine, water, and egg yolks. Horn's research found that lipids are present within the near-infrared regions at 1725, 1762, 2309-2310, and 2347-2352 nm, and proteins are present at 2042-2063 and 2173-2177 nm (Horn 2018). Horn found that carbohydrates in the form of polysaccharides are present at the wavelengths 1692, 1771, 1827, 1923, 2319, and 2352 nm. The results from Horn's research with animal and vegetable fats, animal blood, urine, water, and egg yolks was used as a proxy for human decomposition. The results from Horn's research can be used be used as a proxy because proteins, fats, and carbohydrates are broken down through decomposition and are present in the fluid (Janaway et al. 2009). Because human decomposition fluid is comprised of lipids, carbohydrates, and proteins it is expected that the signature of the fluid will appear on the EMS at the same wavelength values described above.

The CDI has the potential to provide information on how human decomposition fluid interacts with the environment. The effects of human decomposition on the environment allow for the use of FORS to analyze the spectra of plants and soil near a decomposition site. Researching specific spectral bands associated with lipids, proteins, and carbohydrates that are directly associated with decomposition fluid in the spectra of

plants and soil may indicate whether there are any components of decomposition are present. Lipids, carbohydrates, and nitrogen are released from the body as cadaveric materials in the form of purge fluid and deposited onto the soil. The plant roots take up these materials through the soil. The increased presence of lipids, carbohydrates, and proteins from plant leaves and soil decomposition fluid should be detectable using FORS.

CHAPTER THREE

MATERIALS AND METHODS

Materials

The 32 individuals used in this study donated their bodies to the Forensic Anthropology Center (FAC) were placed at the outdoor Anthropology Research Facility (ARF), at the University of Tennessee, Knoxville. About 100 donors are received annually, and over 5,000 individuals are pre-registered for body donation. Upon their death, a donor is transported to the FAC for an intake process before placement at the ARF. Intake includes assessing the donor for applicable research projects and recording information such as cadaver stature and weight. The ARF is an approximately 3-acre wooded area with sloped terrain and a preserved temperate deciduous forest (Cobaugh et al. 2015). The soil profile at the ARF is characterized as very deep, well-drained, clayey soil (Damann et al. 2012). The soil is formed in residuum from interbedded, leached sandstone and shale (Damann et al. 2012). The surface sediments located zero to five centimeters below the surface are comprised of partially decomposed hardwood leaf litter. Five to fifteen centimeters below the surface is a friable, acidic, dark reddish-brown loam with roots present (Damann et al. 2012). The ARF is segmented into different sectors to easily track the location of each individual. Figure 3.1 is a map of ARF that displays the placements site for each donor used in this research.

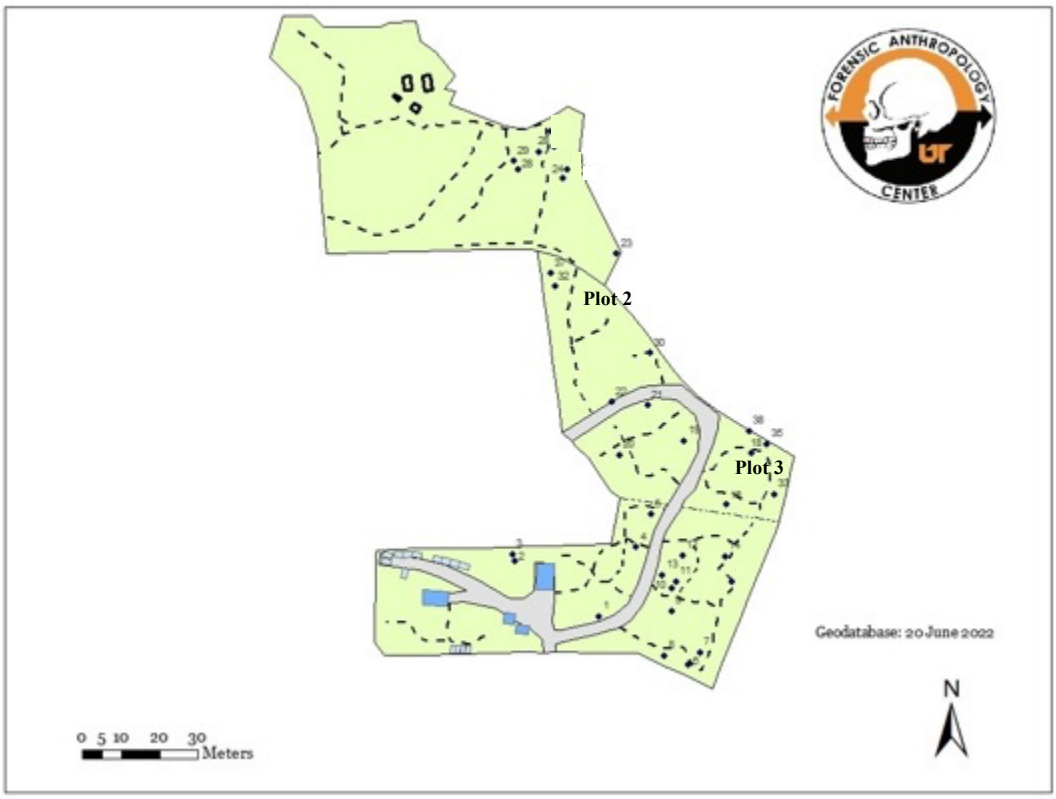

Figure 3.1: Map of donor placements throughout the ARF. The black dots on the map indicate a donor placement site. The black dashes indicate walk paths throughout the sectors.

Of the 32 donors used in this study, 14 are females, and 18 are males. The age range of the donors is between 26 and 91 years (average 69 years) and can be found in Table A.1 in Appendix 1. The donors were placed across each sector of the ARF. Each donor location (Figure 3.1) was selected based on proximity to targeted plants. The soil beneath and surrounding each donor was also used for the research. These 32 donors were divided between two different sample sets (longitudinal and cross-sectional) in order to answer the research questions. The different sample sets and the data collection process for each of these sample sets will be discussed later in this chapter.

Spectroradiometer

Spectral data was collected using a Malvern Panalytical ASD FieldSpec 4 Standard-Res Spectroradiometer (Figure 3.2). The instrument's wavelength range is from 350 to 2500 nm and records spectra based on 2151 wavelength bands (Danner et al. 2015). The resolution varies from 3 nm in the short wavelengths and 10 nm in the longer/farther wavelengths (Danner et al. 2015). This instrument has three different fiber-optic detectors to record the spectra, which include a NIR-enhanced silicon array composed of 512 elements (350-1000 nm) and thermoelectrically cooled indium gallium arsenide (InGaAs) photodiodes for the SWIR1 (1000-1800 nm) and the SWIR2 (1800-2500 nm) (Danner et al. 2015; ASD FieldSpec 4 Brochure; Schweiger 2020). The spectra were collected through the instrument's software RS^3 which is processed on an accompanying laptop. The spectral data was calibrated on a Spectralon White Reference panel with a reflectance value of 1.0 using the internal light source within the contact

probe (Figures 3.2,3.3). Data collection was done using the instrument's contact probe to control for the large canopy and filtered sunlight at the ARF (Milton et al. 2009, Gupta 2018; Muñoz-Huerta et al. 2018). The contact probe houses its own light source, thereby controlling interference from external light from the sun and atmospheric water bands (Milton et al. 2009). The contact probe also ensures that adequate light is available and consistent throughout collections enabling replicable sample data. This allows for standardization at each collection interval, so each leaf receives the same light intensity (Milton et al. 2009). The operating procedures for the instruments used for this research are detailed in Appendix A. Material being sampled for this research includes human decomposition fluid, plant leaves, and surface soil.

Plant Leaves

The leaves from a total of n=57 plants amur honeysuckle (Lonicera maackii) plants were selected for study. Amur honeysuckle was the species selected for this research because of its prevalence at the ARF (Figure 3.4). Amur honeysuckle is a hardy, multi-stemmed deciduous woody scrub that can grow up to 15 to 20 feet high. The leaves of amur honeysuckle are simple, smooth elongated ovate shaped covered in tiny hairs. This species is considered invasive in East Tennessee. Amur honeysuckle has an expansive root system and can respond quickly to a changing environment. Invasive plants response includes changing their chemical make-up based on what they are exposed to in the soil, as well as, affecting the soil chemistry changing the plants performance (Weidenhamer and Callaway 2010, Brabazon et al. 2020, Fahey and Flory

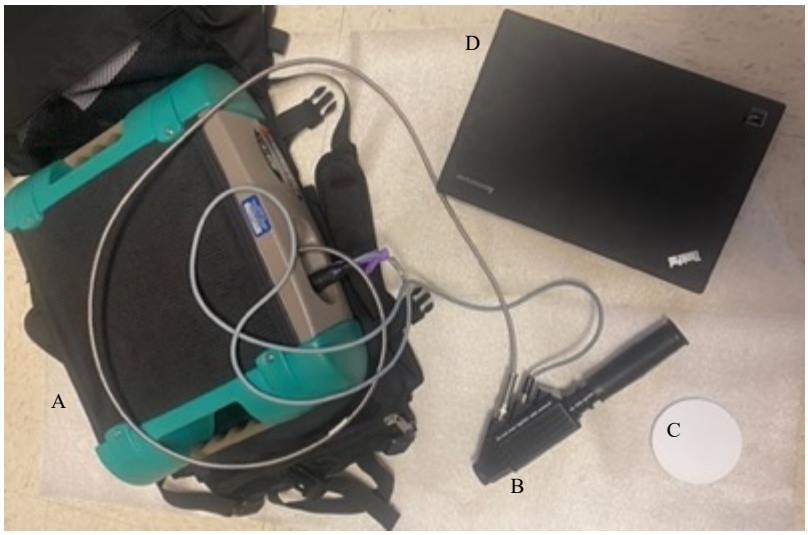

Figure 3.2: ASD Malvern Panalytical FieldSpec 4 Instrument. A: The main component to the instrument that houses the fiberoptic cable. B: The contact probe. C: The Spectralon White Reference. D: Laptop the connects to the instrument that controls the RS^3 software.

Figure 3.3: Contact probe making contact with the Spectralon panel. This is to collect a white reference.

Figure 3.4: An Amur honeysuckle selected for analysis. The purple flagging tape was used to mark this plant with the plant number/plant ID.

2022). Invasive plants species can also alter the soil nitrogen levels (Weidenhamer and Callaway 2010). Plants were chosen based on their proximity to the donor, no plant exceed more than 290cm away from the donor. Prior to data collection all n=54 plants were flagged so that the leaves from the same 54 plants were collected throughout the research. All plant leaf samples were collected by placing the contact probe approximately mid-leaf because this is the area of the leaf that allowed for complete contact of the probe to the leaf. At each collection the leaves randomly selected for sampling. Sampling leaves at random is effective when relating leaf spectra to environmental processes (Schweiger 2020). Figure 3.5 depicts plant spectra collection at ARF using the instrument with the accompanying contract probe for data collection. Leaf samples were collected from the low-lying leaves up to about two meters on the plant. The samples were only taken up to two meters because this is as far as I was able to reach with the contact probe.

Soil

The soil surrounding 29 of the donors was collected. Soil was sampled by placing the contact probe directly on the ground. The contact probe was flush with the soil being sampled. Large leaves and other large organic material were bushed way from the surface of the soil before the sample was collected. Where each soil sample was collected was dependent on the sample set and will be discussed later in this chapter.

Figure 3.5: Plant spectra collected using the ASD FieldSpec 4 at ARF

Sample Sets

To answer my research questions, two sample sets were used for this study: a longitudinal sample set, which included n=5 donors, and a cross-sectional sample that included of n=27 donors (Table A.1). The longitudinal set answers research question 1): does human decomposition fluid have a spectral signature that can be detected from fluids shed from the body in an outdoor environment, and research, question 2): can the spectral signature of human decomposition fluid be detected in both plant leaves and soil during active decomposition? The cross-sectional data sample set answers research question 3): does the spectral signature of human decomposition fluid persist in the plant leaves and soil after the cessation of active decomposition? The comparison of both longitudinal and cross-sectional donors determines the spectral signatures for decomposition, what compounds from decomposition are present in plants and soil, and how these compounds persist.

Longitudinal Sample Set for Research Questions 1 and 2

The five donors were placed in three separate trials and followed throughout 2021. All five donors were frozen when placed on the ground surface. The donors were placed in different sectors of ARF, referred to as Plots Two and Three, marked on the map in Figure 3.1. Each donor was placed within a 3x3m grid which also included the plants and soil targeted for analysis. The goal of this sample set was 1) to determine the spectral signature of decomposition fluid and 2) to determine if decomposition fluid in soil is absorbed by plants and visible in the spectra. In April 2021, one donor was placed

for soil analysis. In June 2021, two donors were placed for plant and decomposition fluid analysis. In September 2021, two donors were placed. One of these donors was used for plant leaf and decomposition fluid analysis and the other donor was used for soil, plant leaf, and decomposition fluid analysis. Spectral data was collected on the leaves of a total of 5 amur honeysuckle plants used in this sample set. Figure 3.6 displays the placement position, slope, plant location, and location of soil samples within each 3x3m grid. Figure 3.6 also displays from which donors decomposition fluid was collected. The slope of each placement site is important because this is the direction that the CDI will expand potentially impacting the plants and soil down-slope from the donor. Control data was collected on the leaves of each plant, and each are of soil prior to donor placement. Spectra was collected at weekly intervals during active decomposition. Following the cessation of active decomposition, data collection occurred bi-monthly. For all samples at each collection interval, samples were taken in the morning with times ranging from 0730 to 1330 to allow for the sun's location consistency. Samples were only taken on dry days; no samples were taken during or after any precipitation.

When collecting data for the longitudinal sample set, samples were labeled with a base number in R^3 that corresponded with the trial number, plot number, sample type (plant, soil, or decomposition fluid), and date the sample was collected (Operating Procedures Appendix A). The base name for each sample also has an incrementing five-digit sample number followed by an .asd extension (R^3 User Manual 2008). The sample beings with the number 00000 and increases by one digit each time a sample is taken.

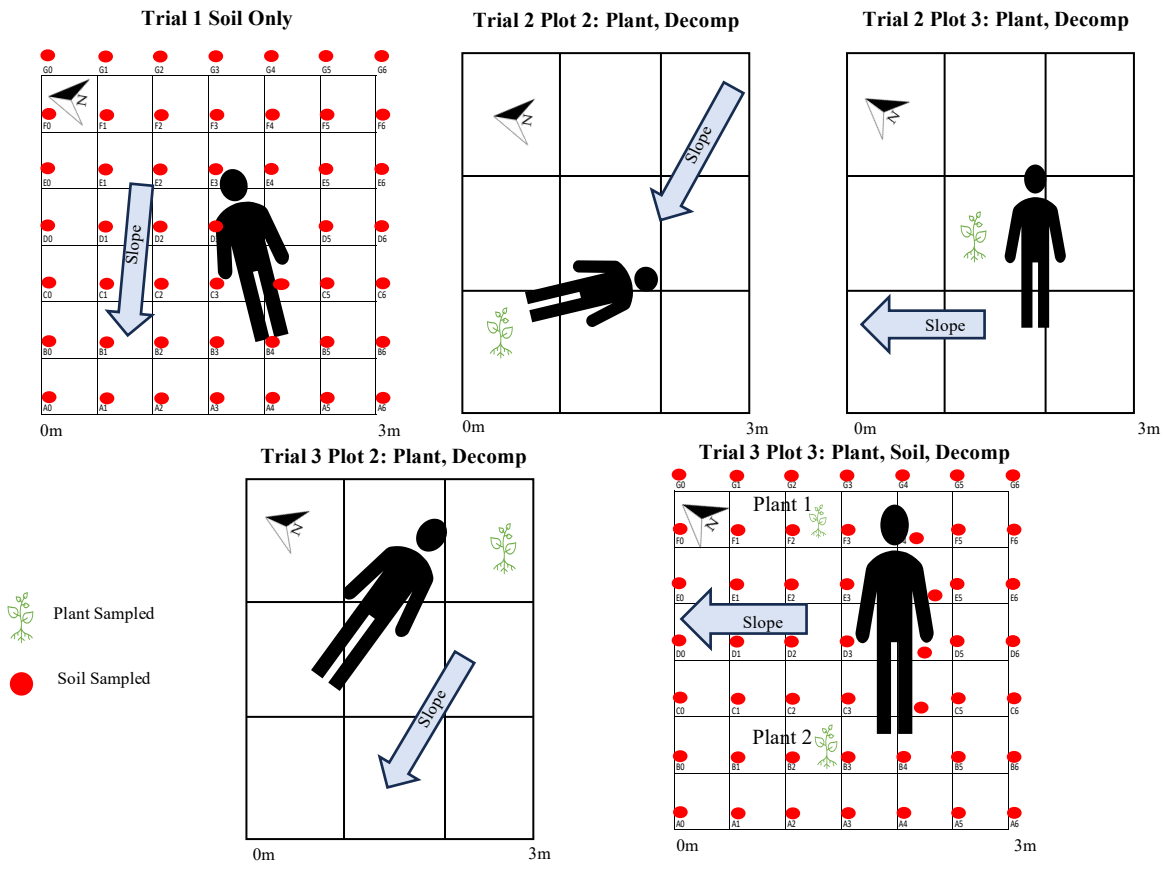

Figure 3.6: Donor, plant, and soil sampling location for each longitudinal donor. For each soil grid the sample ID is listed under the red dot. For the donors with only one plant per plot these are identified as Plant 1. For Trial 3 Plot 3 Donor the plants are identified as either Plant 1 or Plant 2.

An example of the labeling system for a plant would be with the first sample taken as Trial1_Plot2_Plant1_6_2800000.asd and the next would be Trial1_Plot2_Plant1_6_2800001.asd. The incrementing number was how number of samples per collection were tracked.

Decomposition Fluid

Once the donor began releasing decomposition fluid spectral samples were collected. The spectral signature of decomposition fluid was collected by placing the contact probe directly on the decomposition fluid released on the ground surface. The spectra were collected to determine the composition of decomposition fluid. Table A.2 in Appendix 1 displays the samples dates and the decomposition fluid type collected for each donor sampled. Table A.3 in Appendix 1 shows the donors used for the collection of decomposition fluid and the average number of decomposition samples taken. Decomposition fluid was visually characterized into three categories. Viscous decomposition fluid, which was the thick, dense fluid; typically, this is the first sample of decomposition fluid after initial purge (Figure 3.7). This is the concentrated purge fluid. Wet decomposition occurs after viscous decomposition fluid and is characterized by decomposition that is still visibly wet on the surface but is not the thick dense fluid (Figure 3.7). Wet decomposition still has moisture present but is not a concentrated as collection. Dry decomposition fluid, which is decomposition fluid that is still visible on the surface soil but has dried out (Figure 3.7). Dry decomposition occurs after wet decomposition and typically stays the longest on the surface soil.

Figure 3.7: Type of decomposition fluid: A: viscous decomp, B: wet decomp, C: dry decomp

Plant Leaves

Figure 3.6 displays which plots and trials where the five plants were located. Table A.4 found in Appendix 1 displays the sampling dates for the plants per plot in Trials 2 and 3. The plant leaves were followed until November 30, 2021. There were 18 collections for trial two, and nine for trial three. The spectra were collected seven months later, in June 2022, to capture how the plant leaves were affected by the persistence of decomposition fluid in soil and if a similar spectral signature was present after another growing season. Table A.5 displays the average number of spectral samples collected per sampling period for each donor in each trial.

Soil

Two longitudinal donors (Donors 31 and 37) were used to systematically track spectral characteristics of decomposition fluid in the soil (Figure 3.6). The study of these two donors are used to address if the spectra of decomposition fluid is visible in soil during active decomposition. For each of these donors, a separate 3x3m grid was set up and divided into 50-centimeter increments. The grid was placed around each donor. Figure 3.6 display the location and orientation of the donor in each grid. A spectral sample was collected at each 50-centimeter mark for a total of 49 samples per grid. Figure 3.6 displays the location of each sample. When collecting the sample, each sample was labeled with a different letter followed by a number depending on the row. Figure 3.6 displays the lettering system below for each sample. Sample D4 for Donor 31 was not collected after control sampling because the donor was placed over the sampling site.

Therefore, all samplings following the control for Donor 31 only had 48 samples collected. Figure 3.8 displays a grid for Donor 31 and Figure 3.9 for Donor 37. The lines on each grid denote a 50 cm interval. The CDI for each donor was visually tracked at each sampling from initial presentation through the last collection of 2021. The sampling dates for each grid are in Table A.6 in Appendix 1. During collection samples were labeled by trial number, plot number, soil sample letter/number, and date the sample was taken. For example, the sample would be saved at Trial5_Plot3_A4_9_16. The sample would then be followed with the five-digit incrementing number beginning at 00000 indicating the sample number.

Cross-Sectional Sample Set for Research Question 3

The cross-sectional set includes n=27 donors that decomposed at different times on the ground surface (Table A.1). This sample set examines whether decomposition fluid characteristics are visible in the plant spectra after active decomposition stops. In addition to plants, this sample set was also used to examine whether a spectral signature of decomposition persists in the soil, particularly in the groin area, following the cessation of active decomposition. Dates of placements for the donors ranged from years 2017 to 2022. Table A.7 in Appendix 1 includes a list of the donors, their respective placement dates, and plant selected for collections. At the time of data collection, all donors were no longer releasing fluid into the soil and were either mummified or skeletal. Data on these 27 donors were collected in the mornings of June 15, 16, 17, and 22nd. The samples were only collected once on each plant and area of soil. Sampling occurred on

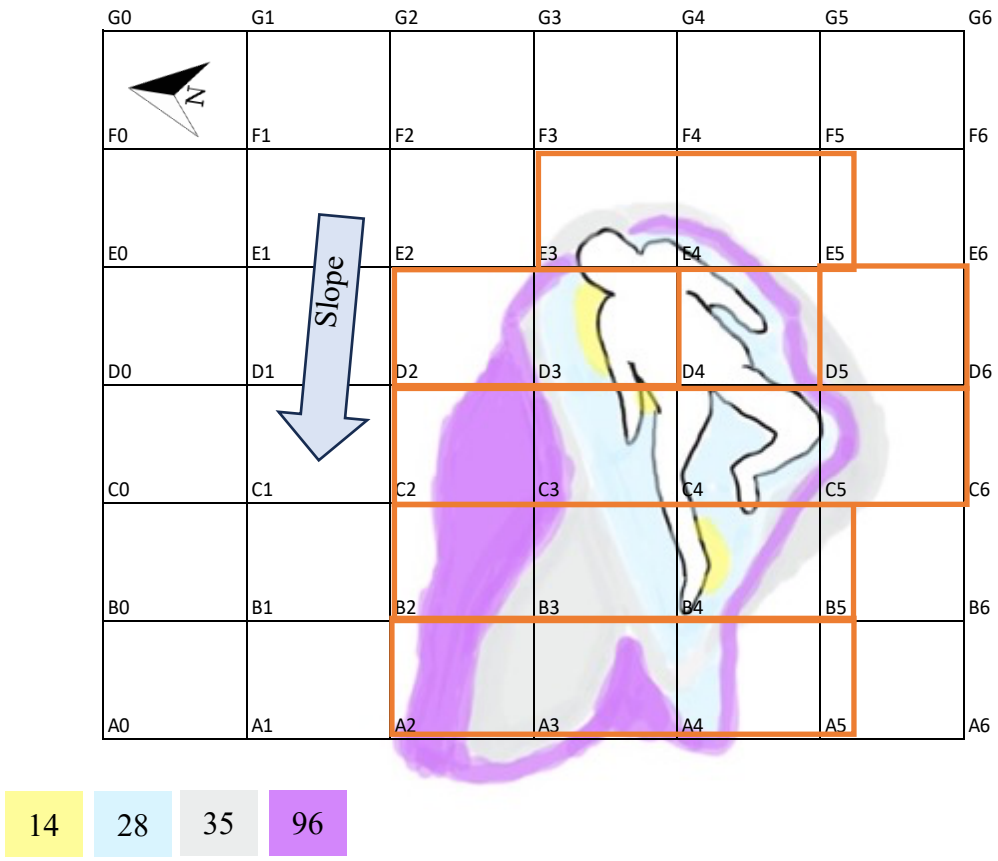

Figure 3.8 Soil grid for Donor 31. Colors indicate the CDI expansion on days 14, 28, 35, 96. The spectra were analyzed from the blocks outlined in orange. The grid is 3x3m and the lines on each grid denote a 50 cm interval. The letter and number system in the corner of each block is the sample ID.

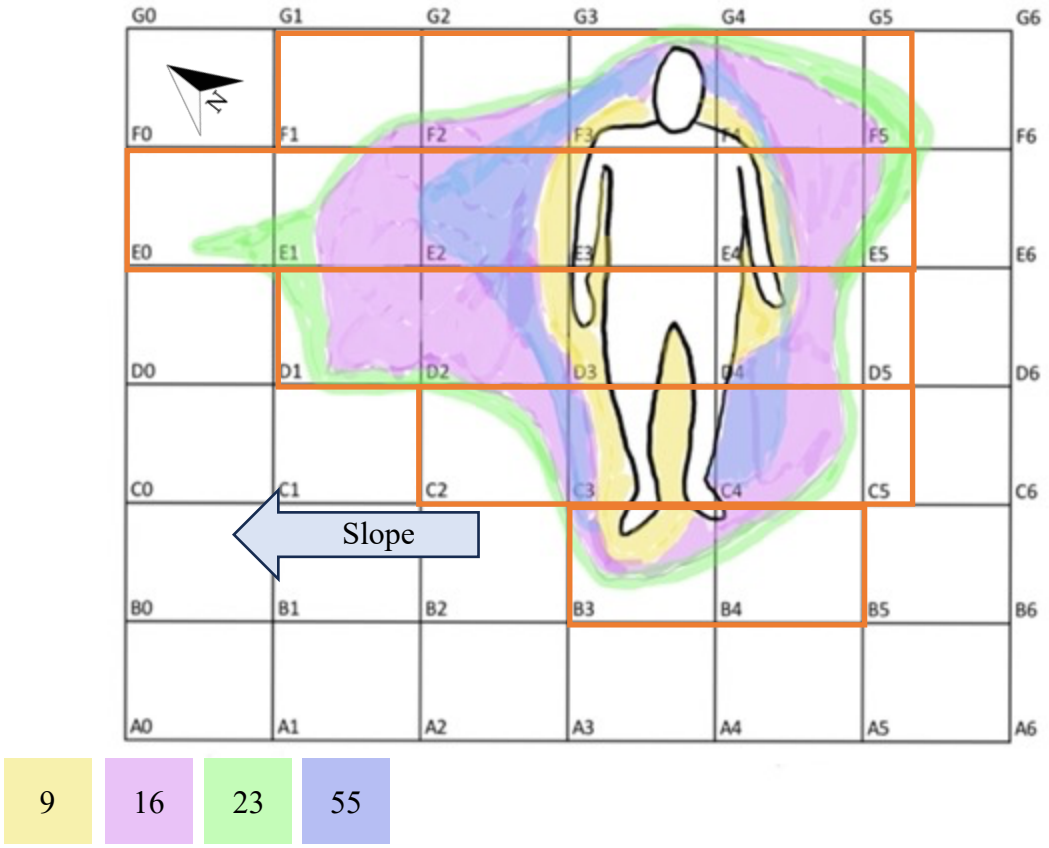

Figure 3.9: Soil grid for Donor 37. Colors indicate the CDI expansion on days 9, 16, 23, 55. The spectra were analyzed from the blocks outlined in orange. The grid is 3x3m and the lines on each grid denote a 50 cm interval. The letter and number system in the corner of each block is the sample ID.

different days with dry and sunny weather conditions because all sampling could not take place over single day. Again, data was collected, in the morning with times ranging from 0730 to 1330 to allow for the sun's location consistency.

When collecting data for the cross-sectional sample set, samples were labeled with a base number in R^3 that corresponded with the donor number and plant number for the plant samples. For soil samples the labeled would be comprised of the donor number and soil (Operating Procedures Appendix A). For example, the labeled for Donor 1, Plant 1.1 would look like Donor 1_Plant1.100000.asd followed by Donor 1_Plant1.100001.asd. For soil, the sample would be labeled as Donor 21_Soil.

Plant Leaves

Control data was collected on the leaves from two amur honeysuckle plants in an area outside of the ARF that had not been previously impacted by human decomposition. These plants were located in a new area outside of ARF. Two plants were selected as controls due to the available plants in this area. For each control plant, a spectrum was collected from approximately 100 leaves and during collection the samples were labeled by plant number. There are 49 total plants sampled in the cross-sectional sample set. The number of plants selected per donor varied depending on the available amur honeysuckle near a donor placement site. The plants were chosen based on the proximity to the donors. The donors will have either one or two plants sampled. Table A.7 in Appendix 1 displays each donor's plant and how they were labeled for collection purposes. The

distance from the plant to the donor was taken from the groin and the distances are listed in Table A.7.

For each plant, a spectrum from approximately 100 leaves was collected. Each spectral sample was taken on different leaves that were randomly selected at the time of collection. For plant 8.2, there were not 100 total leaves on the plant, so multiple samples were taken per leaf to obtain approximately 100 samples. The samples were randomly taken on leaves across the whole plant where leaves were reachable with the contact probe.

Soil

Control data for cross-sectional soil was collected in two separate areas of soil. These areas of soil were taken in an area outside of ARF that had not previously been impacted by decomposition fluid. For both areas of soil approximately 30 spectra were taken at each site. For each of the 27 donors in this sample set, approximately 30 spectra of the soil within the groin region were taken at each sampling period. The groin was chosen for the area of soil analysis as this is an area where a large amount of decomposition fluid is released from the body.

Initial Data Processing

After each collection day for both the longitudinal and cross-sectional sample sets, data was copied from the instrument's laptop on to an external hard drive. All spectral data collected with the ASD FieldSpec 4 was then processed using Fisher

ThermoScientific GRAMS IQ software. This software views spectral data to create a calibration file containing the mean averages for each spectral band (350-2500 nm). The ASD FieldSpec 4 saves each spectrum as an .asd file; however, each file had to be converted to a .spc file for analysis. Indico Pro version 6.0 was used for each file conversion. The Log 1/R file conversion was used because this data conversion is ideal for GRAMS IQ to create the calibration file (GRAMS IQ manual v9.1). A calibration file was created for each collection date per sample type (plant leaves, soil, or decomposition fluid). Before creating the calibration files, the data was analyzed for any outliers due to a poor-quality spectral sample that occurred during sampling. Poor-quality spectra were assessed visually based on the overall reflectance values. Visually evaluating the quality of the spectra ensured that the data, specifically the control data, was within the limits of normal variation. Initially each calibration file created contained the means for all bands (300-2500 nm); however, the means used for analysis was reduced to only 62 bands which will be discussed later in this chapter.

Longitudinal Samples

The data collected from the decomposition fluid, plant leaves, and soil in this sample set was used to create the calibration flies for analysis. The decomposition spectra have an average of 20-25 spectra per average used in the calibration file (Table A.3). Each longitudinal plant sample has an average of 69-71 leaf spectra per sample used in each calibration file. Unless it was clear that the plants in the longitudinal sample had a

poor-quality spectral sample, due to error when collecting, all samples were included as the difference could be from the impact of decomposition fluid.

The soil samples chosen for spectral analysis were targeted in the 50cm blocks from the 3x3m grid where the CDI expanded. These blocks are displayed in Figures 3.7 and 3.8. All the samples from each block per sampling date were combined together when creating the calibration files; therefore, the results reflect the average from all the blocks per sampling. Calibration flies were collected with the combined blocks for each collection day. The spectra in each calibration file were visually assessed for a poor-quality spectral sample, due to error when collecting. Unless it was clear that the sample collected was of poor- quality all samples were included.

Cross-Sectional Samples

Plant

For each plant in the cross-sectional data set, there are 100 spectra used in the calibration files. More than 100 spectra were collected from each plant, but only 100 were used for analysis. To reach 100 spectral samples the spectra were either removed by visually assessing them to be poor quality based on their reflectance values or if all were visually of good quality, they were randomly removed to reach 100 samples for each calibration file. Once 100 spectra were present for each plant a separate calibration file was created for each plant to be used for analysis.

Soil

Calibration files were created for the soil samples in the cross-sectional sample set using the same process that was used to calibration files for the cross-sectional plant samples. During collections for each donor more than 30 soil spectra were collected. To reach 30 spectral samples the spectra were either removed by visually assessing them to be poor quality based on their reflectance values or if all were visually of good quality, they were randomly removed to reach 30 samples for each calibration file.

Calibration Files and Statistical Analysis

The calibration files were created in GRAMS IQ using a discriminate, cross-validation model and multiplicative scatter pathlength correction (MSC). A discriminate calibration model is used for developing qualitative calibration files. A cross-validation diagnostic type provides an estimate of the prediction error when unknown samples of a similar type are predicted with the model. An MSC pathlength correction normalizes each spectrum to an 'ideal spectrum' which is assumed to be the average of all the spectra. MSC is calculated by a regression of each spectrum against an ideal spectrum. The correction is then performed individually over each band (GRAMS IQ Manual v.9.1).

To answer my research questions, a Principal Component Analysis (PCA) was used based on 62 selected bands. Sixty-two bands were selected that include areas where decomposition fluid characteristics are expected to be present for lipids, carbohydrates, and proteins. Table A.8 in Appendix 1 lists all bands selected for inclusion in the

statistical analysis. Each spectrum provides a large amount of data for each band; therefore, a PCA was selected because it is able to simplify the large datasets and identify recurring patterns with little loss of information (Beattie and Esmonde-White 2021). Reducing the number of bands avoids the potential of comparing bands that create noise within the spectrum, resulting in a distortion of the results creating false positives (Beattie and Esmonde-White 2021). To perform the PCA analysis, the means for each band from each calibration file created were transposed into .csv files. The PCA was preformed using R software with the Vegan package. The PCA process organizes the information between the variables to explain information in order of magnitude and prevalence (Beattie and Esmonde-White 2021). PC1 and PC2 hold the largest amount of information and correlate strongly to chemical features in the bands which can include molecular concentration and physical properties of the sample (Beattie and Esmonde-White 2021).

Decomposition Fluid Analysis

A .csv file was created the contained only the 62 selected bands for each calibration file. The .csv file for only decomposition fluid contained the means for the decomposition fluid spectra from all donors. The 62 bands selected were divided by columns and the means from each collection day were divided by row. The sample type (viscous, wet, or dry) was designated for each collection day. The decomposition type was abbreviated to VD for viscous decomposition, WD for wet decomposition and DD for dry decomposition. The .csv file was then imported in R where the PCA analysis was performed.

Longitudinal Plant Analysis

A .csv file for each plant per trial and plot was created that contained only the 62 selected bands for each calibration file. The .csv file for the longitudinal plants contained means from all decomposition fluid and the means for the plant per collection day. The 62 bands selected were divided by columns and the means from each plant collection were divided by row. The decomposition fluid sample type (VD, WD, DD) was designated for each collection day, the control samples were given the sample type of C, and all samples collected after placement were given the designation of T for test samples, and the samples that were collected in June 2021 was given the designation of J. The .csv file was then imported in R where the PCA analysis was performed.

Longitudinal Soil Analysis

A .csv file for each area of soil per trial and plot was created that contained only the 62 selected bands from each calibration file. The .csv file for the longitudinal soil samples contained means from all decomposition fluid and the means for the soil per collection day. The 62 bands selected were divided by columns and the means from each soil collection were divided by row. The decomposition fluid sample type (VD, WD, or DD) was designated for each collection day, the control samples were given the sample type of C, and all longitudinal soil samples collected after placement were given the designation of T for test samples. The .csv file was then imported in R where the PCA analysis was performed.

Cross-sectional Plant Analysis

A .csv file was created that contained only the 62 selected bands for each calibration file and each plant in the cross-sectional data set. The .csv file for the cross-sectional plants contained means from all decomposition fluid and the means for the plant. The 62 bands selected were divided by columns and the means from each plant collection were divided by row. The decomposition fluid sample type (VV, WD, or DD) was designated for each collection day, the plant control samples were given the sample type of C, and all other plants samples collected were given the designation of T for test samples. The .csv file was then imported in R where the PCA analysis was performed.

Cross-Sectional Soil Analysis

A .csv file that contained only the 62 selected bands for each calibration file and each area of soil in the cross-sectional set. The .csv file for the cross-sectional soil samples contained means from all decomposition fluid and the means for each area of soil. The 62 bands selected were divided by columns and the means from soil collection were divided by row. The decomposition fluid sample type (VD, WD, DD) was designated for each collection day, the control soil samples were given the sample type of C, and all soil samples collected after placement were given the designation of T for test samples. The .csv file was then imported in R where the PCA analysis was performed.

CHAPTER FOUR

RESULTS

Human decomposition fluid is comprised of lipids, carbohydrates, and proteins. Areas on the EMS that correspond to these materials were targeted for analysis. This chapter first provides example spectra of decomposition fluid highlighting the location of lipids, carbohydrates, and proteins. The spectra of plants, soil, and decomposition fluid are compared to highlight the differences in absorption and reflectance values for each sample type. Next, the chapter will discuss the PCA results for the longitudinal sample set for decomposition fluid, plants, and soil. Finally, the chapter will detail the PCA results for the cross-sectional sample set for both plants and soil.

The goals of this study are to determine if human decomposition fluid has a detectable spectral signature that can be identified in plants and soil and whether that signature persists. Figures 4.1 and 4.2 provide examples of how each spectral type appears when collected. Specifically, Figure 4.1 illustrates, decomposition fluid spectra and highlights the bands selected for statistical analysis. The peaks highlighted at approximately 1600-1900 nm represent lipids and carbohydrates. At approximately 2000-2200 nm, the peaks indicate proteins; at approximately 2300-2400 nm the peaks account for lipids. Figure 4.2 illustrates decomposition fluid, plant leaf, and soil spectra. The plant leaf and soil spectra are from control samples. The decomposition spectra exhibit a higher reflectance value than both plants and soil, while plants exhibit a higher reflectance value than soil. For the plant spectra, typically 600-1350 nm accounts for

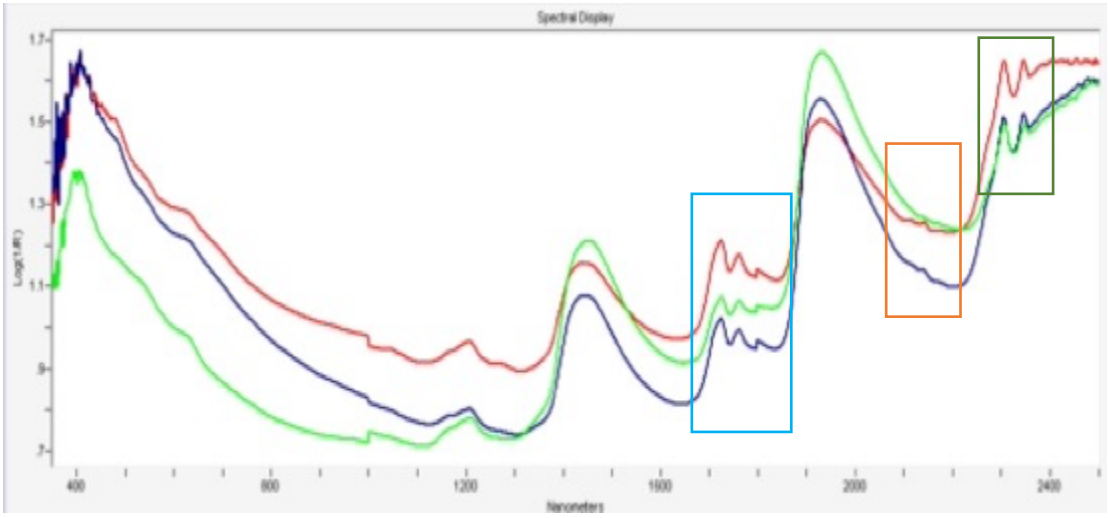

Figure 4.1: Decomposition fluid spectra from three samples during active decomposition. The blue box highlights bands representative of lipids and carbohydrates. The orange box highlights bands representative of proteins. The green box highlights bands that is representative of lipids.

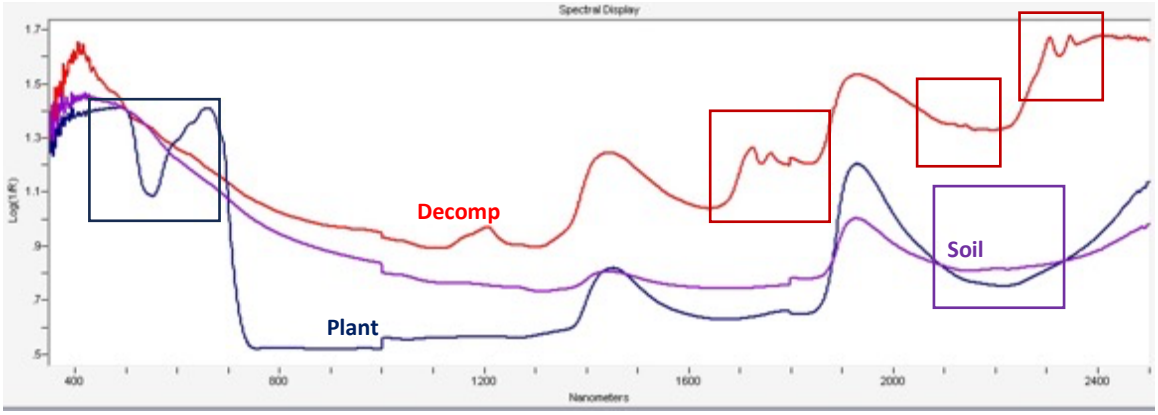

Figure 4.2: Plant, soil, and decomposition fluid spectra. Note the differences in reflectance value on the y-axis, and the areas of absorption features. The blue box indicates the area of absorption feature for plant leaves. The purple box indicated indicates the area of absorption feature for soil. The red boxes indicate the area of absorption feature for human decomposition fluid.

plant health. For soil spectra, typically between 2000-2300 nm are characteristics of interest. The primary research questions here focus on detecting decomposition fluid in plant leaves and soil, therefore, only certain bands between 1692-2354 nm were selected for statistical analysis (Table A.8).

To specifically address research question 1, whether human decomposition has a detectable spectral signature, a PCA using spectra from all decomposition fluid from trials 2 and 3 were conducted. To answer, research question 2, whether the spectral signature of human decomposition can be detected in plant leaves and soil during active decomposition, the means from the spectra collected from the leaves of each plant and the means from the selected soil spectra were analyzed using PCA. The mean spectra of the decomposition fluid spectra were also used in the PCA to identify any groupings between the plants or soil and decomposition fluid. The results from these analyses are discussed below. Finally, to address research question 3, whether human decomposition fluid has a detectable spectral signature that persists after the cessation of active decomposition, a PCA using the cross-sectional data set and all decomposition data was completed. The purpose of this analysis is to identify any groupings between the decomposition fluid and the plant leaf or soil spectra.

Results for Longitudinal Sample Set for Research Questions 1 and 2

To address research question 1): does human decomposition fluid have a

detectable spectral signature that can be found fluids shed from the body in an outdoor environment, decomposition fluid was analyzed from four donors (Figure 3.6).

Decomposition Fluid

Decomposition fluid was divided into three groups, viscous, wet, and dry decomposition fluid (Figure 3.7). Figure 4.3 displays an example of the spectra for each type of decomposition fluid collected. Depending on the type of decomposition fluid collected the reflectance values differ. Viscous decomposition fluid has the highest reflectance value, with pronounced lipid, carbohydrates, and lipid bands. Viscous decomposition fluid also has decreased water bands indicating that there is less water content present, displaying that the lipids, carbohydrates, and proteins account for the variation in reflectance. The wet decomposition fluid spectra reflect less than viscous decomposition fluid, with more pronounced water bands and less pronounced lipids, carbohydrates, and proteins. Wet decomposition fluid is expected to have increased water bands because of the moisture content relative to the lipid, carbohydrate, and protein concentration. The dry decomposition fluid spectra have decreased reflectance than both the viscous and wet decomposition fluid spectra with less pronounced reflectance of the lipids, carbohydrates, and proteins. This indicates that the concentration of these materials is not as high or do not have as strong of a reflectance as what is seen in the viscous decomposition.

The results of the PCA for decomposition display variability among the decomposition samples (Figure 4.4). Decomposition fluid of the same type does not

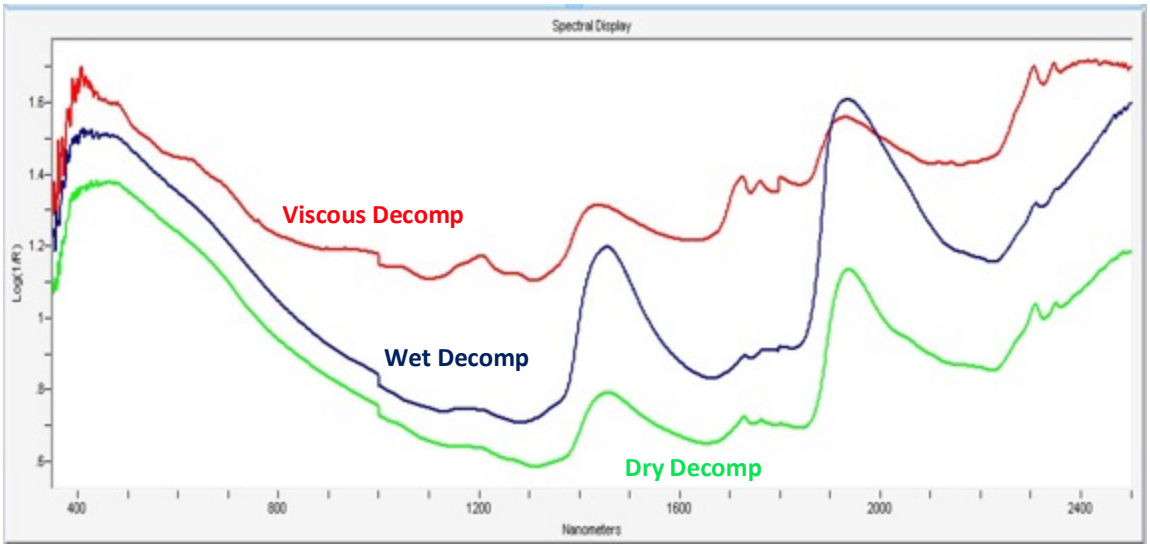

Figure 4.3: Difference in spectra of viscous, wet, and dry decomposition fluid. Note the difference in reflectance values on the y-axis and the concentration of lipids, carbohydrates, and proteins between 1600-2400 nm for each type of fluid.

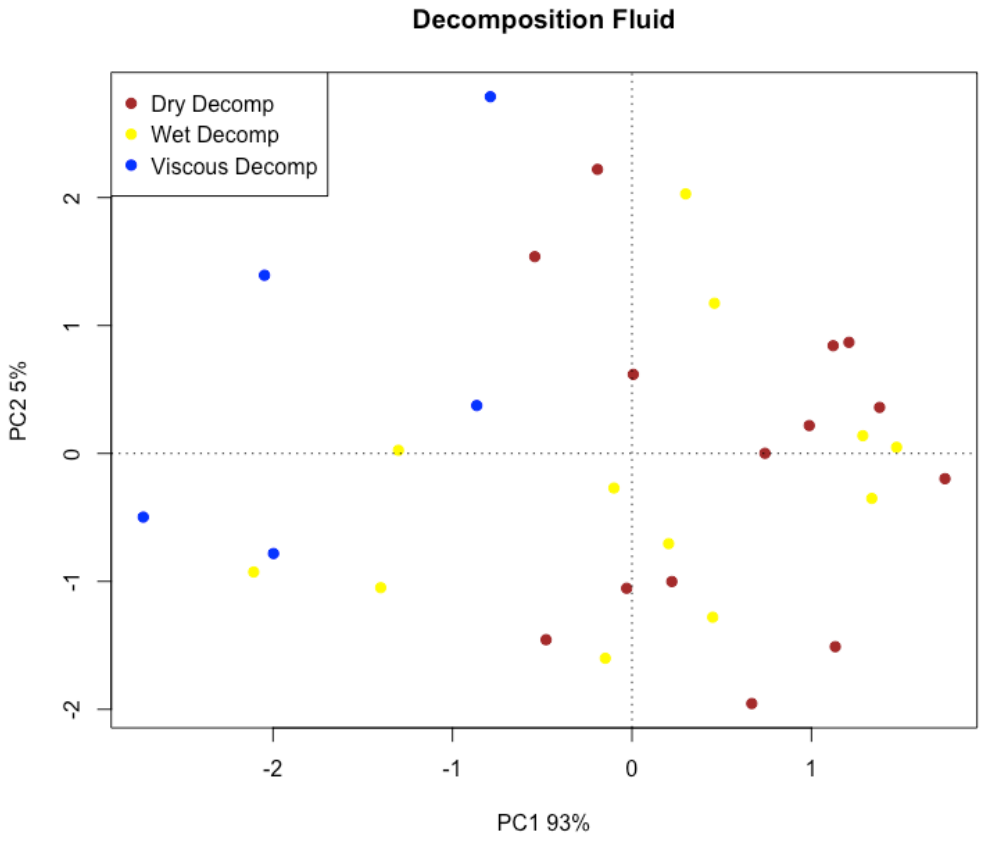

Figure 4.4: PCA of all decomposition fluid for Donors 33, 34, 36, 37. Note that each type of fluid is dispersed across both PC1 and PC2. There are no groupings among any type of fluid. The bands that account for the variation among the samples in PC1 are 2354 nm, 2352 nm, and 2353 nm and are indicative of carbohydrates. The bands that account for the variation among the samples in PC2 include 1690 nm, 1691 nm, 1692 nm, 1693 nm, and 1694 nm and are indicative of lipids.

group. None of the decomposition fluid is grouped together. Instead, samples are dispersed across PC1 and PC2. PC1 accounts for 93% of the variability. The bands associated with highest variability within PC1 are 2354 nm, 2352 nm, and 2353 nm. PC2 accounts for 5% of the variability and the bands associated with the highest variability of PC2 include 1690 nm, 1691 nm, 1692 nm, 1693 nm, and 1694 nm. Bands in PC1 are related to carbohydrates and the bands in PC2 are related to lipids. Based on the results of this PCA decomposition fluid spectra are inconsistent among or between types. The inconsistency of decomposition fluid could be related to the concentration of each cadaveric material present in the fluid at the time of sampling and the water content.

Plant Leaves

To address whether human decomposition can be detected in plant leaves during active decomposition, the results from each PCA for each plant sampled are displayed in Figures 4.5-4.9. Figure 4.10 depicts the results from all plant leaf samples combined. The results from each PCA indicate that the bands that primarily account for the variation in PC1 are 2170-2174 nm and the bands that account for the variation in PC2 are 2040-2043 nm. The bands associated with both PCs indicate proteins. These bands have the highest means from the calibration files, accounting for the most concentration of reflectance present for the spectra. All decomposition fluid was compared to the plant leaf samples in each PCA. The PCA results for all longitudinal plant leaves are similar. Each result shows that PC1 primarily accounts for the variation in the spectra of the plant samples, while PC2 displays the variation in decomposition fluid (Figures 4.5-4.9). All of the plant

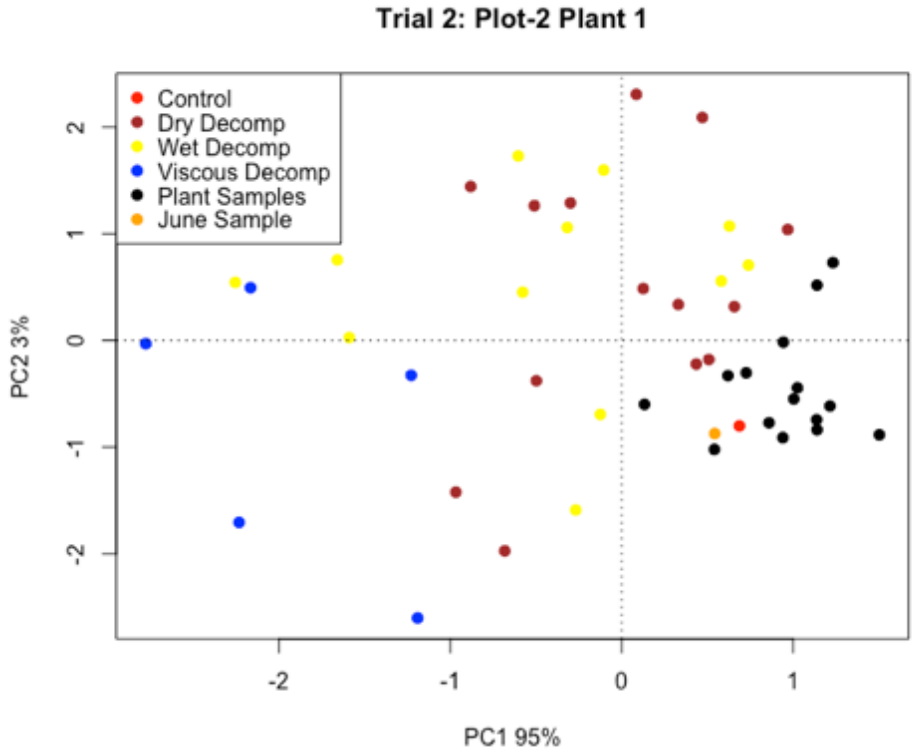

Figure 4.5: PCA for all decomposition fluid and the leaves from Trial 2: Plot-2 Plant 1. Note that the plant leaf samples including the control group together primarily in PC1 while all types of decomposition fluid are dispersed throughout PCs 1 and 2. There is no grouping of plant leaves with decomposition fluid indicating that there is no concentration of lipids, carbohydrates, or protein in the leaf samples at the selected bands. The bands that account for the variation among the samples in PC1 are 2170-2174 nm. The bands that account for the variation among the samples in PC2 are 2040-2043 nm. The bands associated with both PCs indicate proteins.

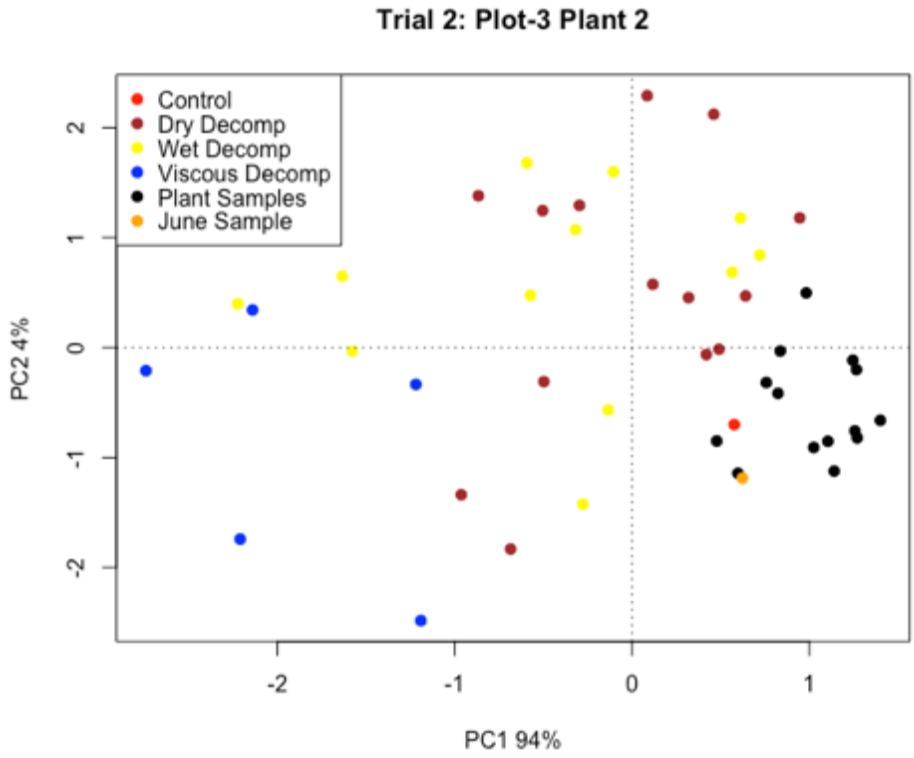

Figure 4.6: PCA for all decomposition fluid and the leaves from Trial 2: Plot-3 Plant 2. Note that the plant leaf samples including the control group together primarily in PC1 while all types of decomposition fluid are dispersed throughout PCs 1 and 2. There is no grouping of plant leaves with decomposition fluid indicating that there is no concentration of lipids, carbohydrates, or protein in the leaf samples at the selected bands. The bands that account for the variation among the samples in PC1 are 2170-2174 nm. The bands that account for the variation among the samples in PC2 are 2040-2043 nm. The bands associated with both PCs indicate proteins.

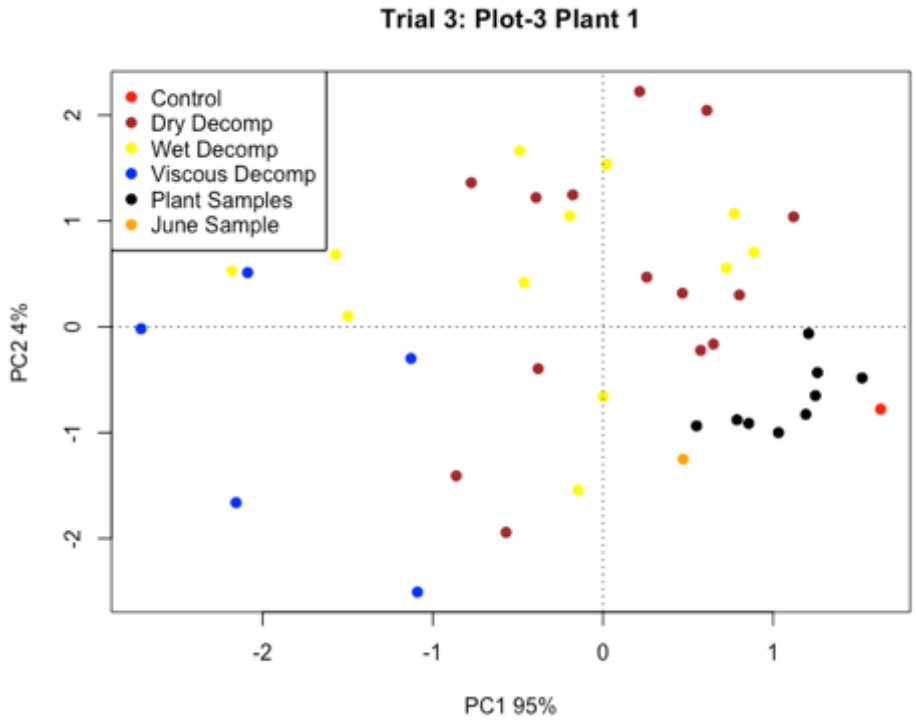

Figure 4.7: PCA for all decomposition fluid and the leaves from Trial 3: Plot-2 Plant 3. Note that the plant leaf samples including the control group together in PC1 while all types of decomposition fluid are dispersed throughout PCs 1 and 2. There is no grouping of plant leaves with decomposition fluid indicating that there is no concentration of lipids, carbohydrates, or protein in the leaf samples at the selected bands. The bands that account for the variation among the samples in PC1 are 2170-2174 nm. The bands that account for the variation among the samples in PC2 are 2040-2043 nm. The bands associated with both PCs indicate proteins.

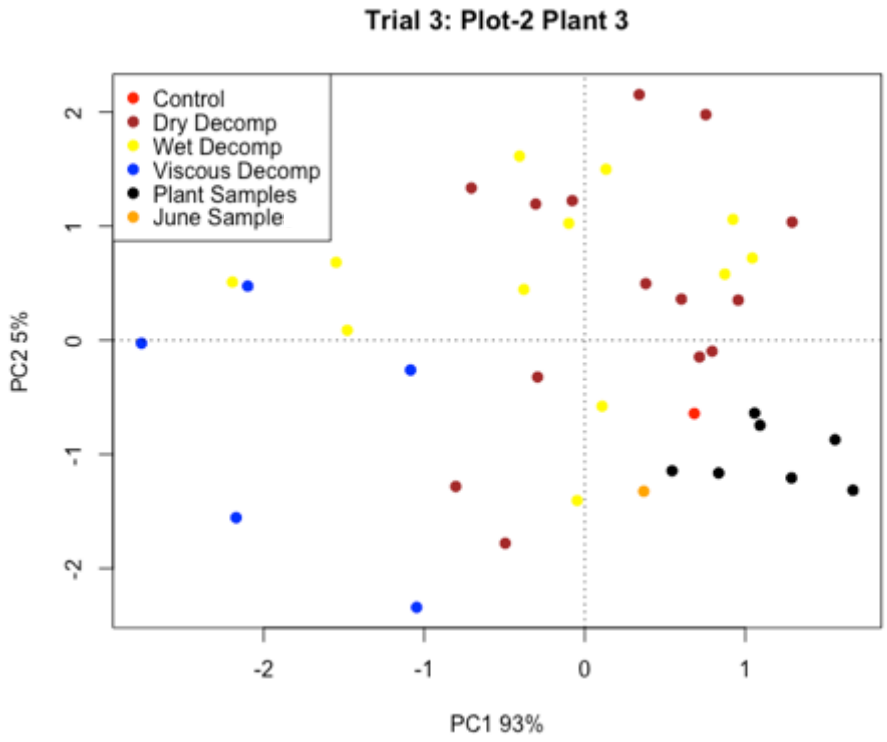

Figure 4.8: PCA for all decomposition fluid and the leaves from Trial 3: Plot-3 Plant 1. Note that the plant leaf samples including the control group together in PC1 while all types of decomposition fluid are dispersed throughout PCs 1 and 2. There is no grouping of plant leaves with decomposition fluid indicating that there is no concentration of lipids, carbohydrates, or protein in the leaf samples at the selected bands. The bands that account for the variation among the samples in PC1 are 2170-2174 nm. The bands that account for the variation among the samples in PC2 are 2040-2043 nm. The bands associated with both PCs indicate proteins.

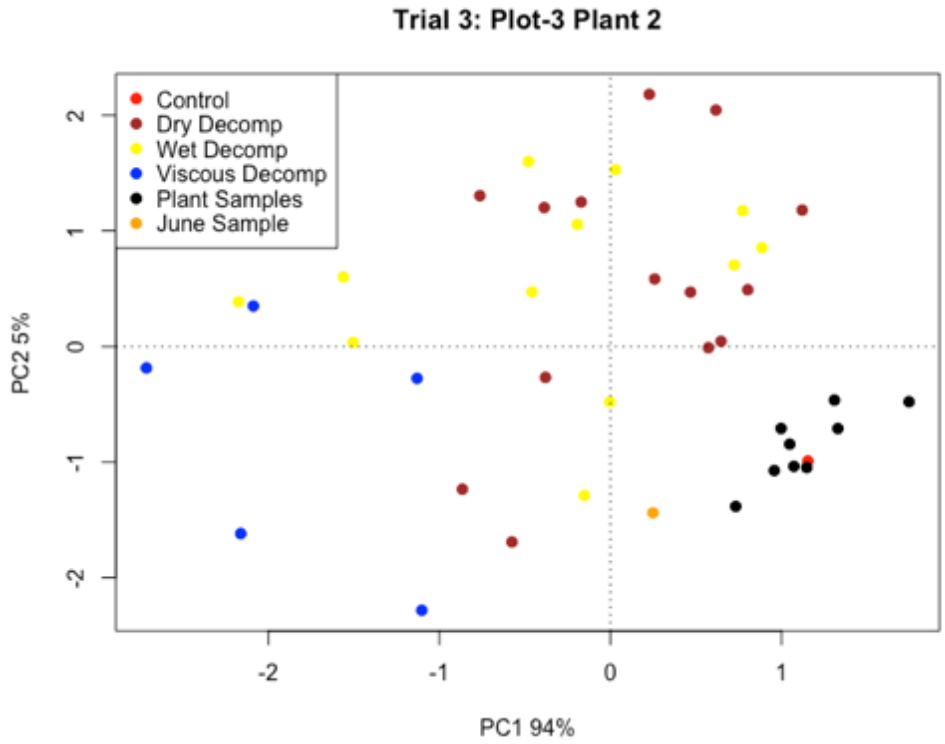

Figure 4:9: PCA for all decomposition fluid and the leaves from Trial 3: Plot-3 Plant 2. Note that the plant leaf samples including the control group together in PC1 while all types of decomposition fluid are dispersed throughout PCs 1 and 2. There is no grouping of plant leaves with decomposition fluid indicating that there is no concentration of lipids, carbohydrates, or protein in the leaf samples at the selected bands. The bands that account for the variation among the samples in PC1 are 2170-2174 nm. The bands that account for the variation among the samples in PC2 are 2040-2043 nm. The bands associated with both PCs indicate proteins.

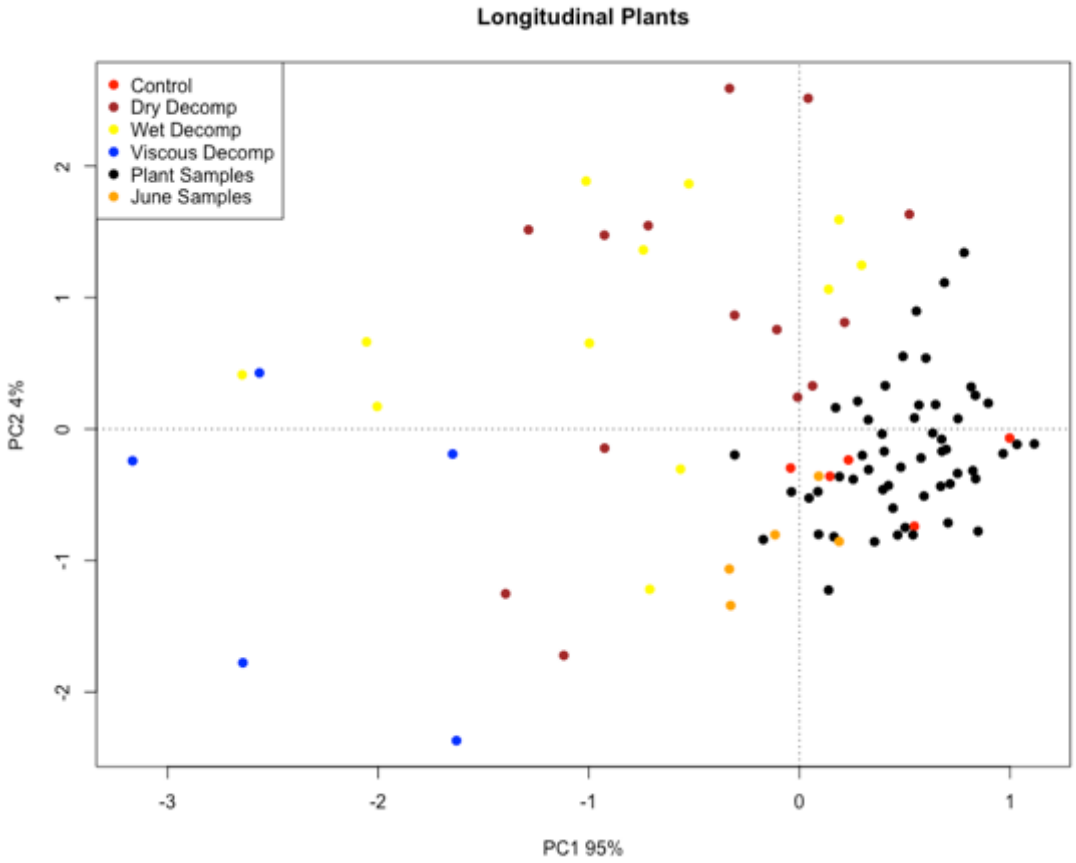

Figure 4.10: PCA for all decomposition fluid and the leaves from all longitudinal plants. Note that the plant leaf samples including the controls group together in PC1 while all types of decomposition fluid are dispersed throughout PCs 1 and 2. There is no grouping of plant leaves with decomposition fluid indicating that there is no concentration of lipids, carbohydrates, or protein in the leaf samples at the selected bands. The bands that account for the variation among the samples in PC1 are 2170-2174 nm. The bands that account for the variation among the samples in PC2 are 2040-2043 nm. The bands associated with both PCs indicate proteins.

leaf samples taken at each collection, including the control samples group together in PC1, while the decomposition is dispersed among PC1 and PC2. This indicates that they do not have concentrations of lipids, carbohydrates, and proteins similar to human decomposition fluid. Comparing all longitudinal data used to answer research question 2 increases the sample size of the PCA. Still, it yields similar results to the PCAs of the leaves of each plant. In the PCA with all data (Figure 4.10), the plant leaf spectra group together, and the spectra of decomposition fluid are dispersed throughout PC2. Because the plant leaves group together, but not with any decomposition fluid type there is no similarity between the plants or the decomposition fluid. These results indicate that plant leaves do not metabolize the lipids, carbohydrates, and proteins that are detectable spectrally during active decomposition.

Soil

The soil samples chosen for spectral analysis were targeted in the 50 cm blocks from the 3x3 m grid where the CDI expanded (Figures 3.8 and 3.9). All the samples from the selected blocks for analysis per sampling date were group together for analysis when creating the calibration files. By grouping the sampling blocks together, the results of the PCA reflect the average from all the selected blocks. For the soil samples from Donor 31, PC1 primarily accounts for the variation among bands 2170-2174 nm and 2040-2041 nm, which indicate proteins (Figure 4.11). The variation in PC2 is among bands 1724-1726 nm, reflecting lipids. However, the results from Donor 37 indicate that PC1 still accounts

for the most variation among bands 2170-2174 nm, while PC2 accounts for variation among bands 2040-2045 nm (Figure 4.12). These bands are all associated with proteins.

The results from Donor 31 indicate that decomposition fluid is not detectable in the soil spectra analyzed. The soil spectra, including the control sample, group together while the decomposition fluid spectra are dispersed throughout PC2. The soil samples do not closely group together, and they also do not group with decomposition fluid. These results indicate that there are not enough concentrations of lipids, carbohydrates, and proteins in the soil samples that are detectable during active decomposition. The variation in the grouping of the soil samples is not due to decomposition characteristics, but rather due to variation in the soil composition.

The results for Donor 37 do show that decomposition fluid, both wet and dry, is detectable in soil. The control soil is separated from the other soil samples taken after donor placement. The samples obtained on 12-Oct-21, 19-Oct-21, 1-Nov-21, 16-Nov-21 and 16-June-21 group with dry and wet decomposition fluid. This grouping indicates that the soil spectra taken on these dates exhibit high enough concentrations of cadaveric materials that can be detected spectrally as decomposition fluid. Figure 4.13 illustrates soil spectra where peaks at the bands selected from decomposition are visible. The difference between Donor 31 and 37 could be due to the concentration of decomposition fluid released from the body which is attributed to body size (Roberts et al. 2017, Mason et al 2022). A larger sample size would be needed to address further why there is a difference between the two donors.

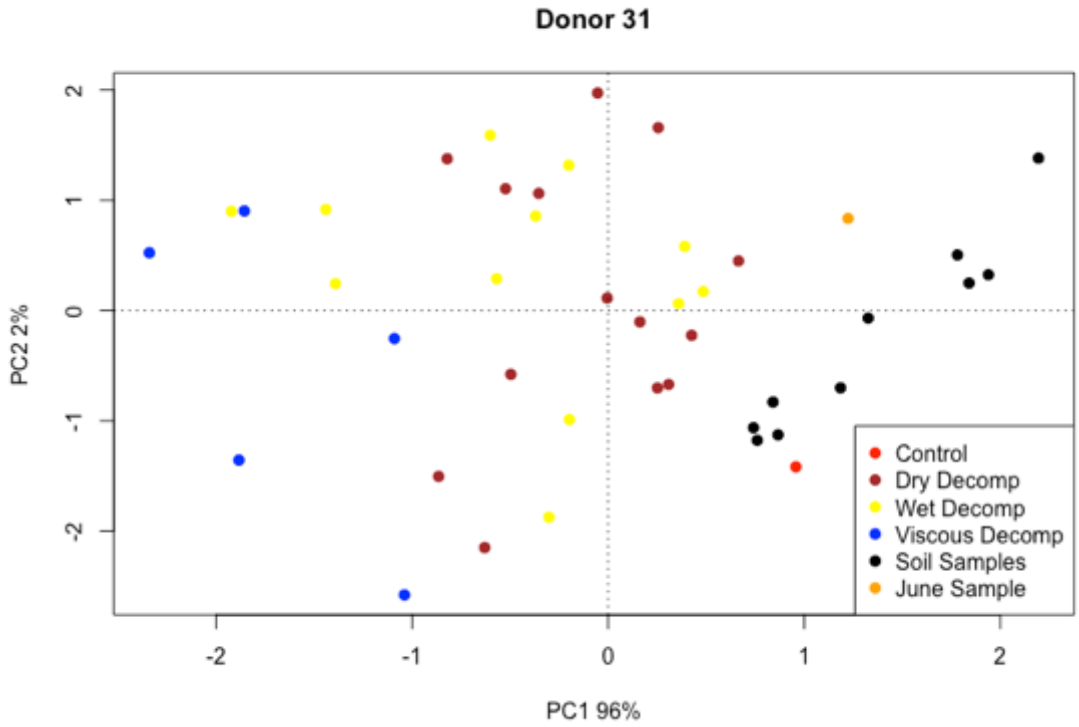

Figure 4.11: PCA for all decomposition fluid and soil for Donor 31. Note that while the soil samples are not closely grouped, they are also not grouped with decomposition fluid. This indicates that there are not enough concentrations of lipids, carbohydrates, and proteins in the soil samples that are also detectable during active decomposition. The bands that account for the variation among the samples in PC1 are 2170-2174 nm which indicate proteins. The bands that account for the variation among the samples in PC2 area 2040-2041 nm which indicate lipids.

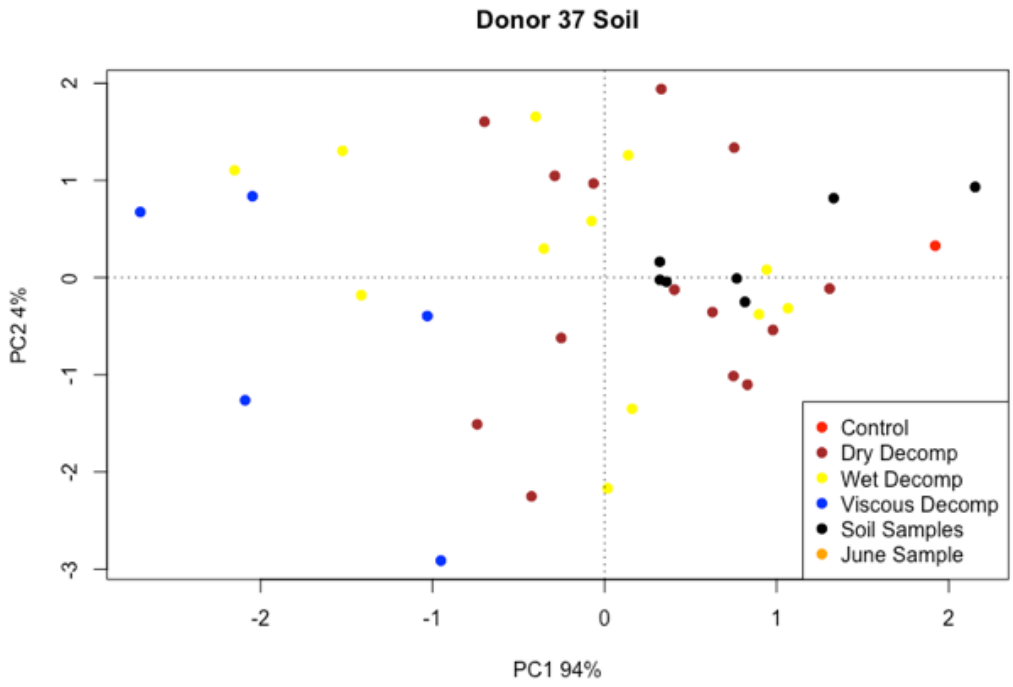

Figure 4.12: PCA for all decomposition fluid and soil for Donor 37. Note that the control sample and two other soil samples do not group with decomposition fluid. These are the first three samples collected. The following five samples collected both wet and dry decomposition fluid. The bands that account for the variation among the samples in PC1 are 2170-2174 nm. The bands that account for the variation among the samples in PC2 are bands 2040-2045 nm. These bands are all indicative of proteins.

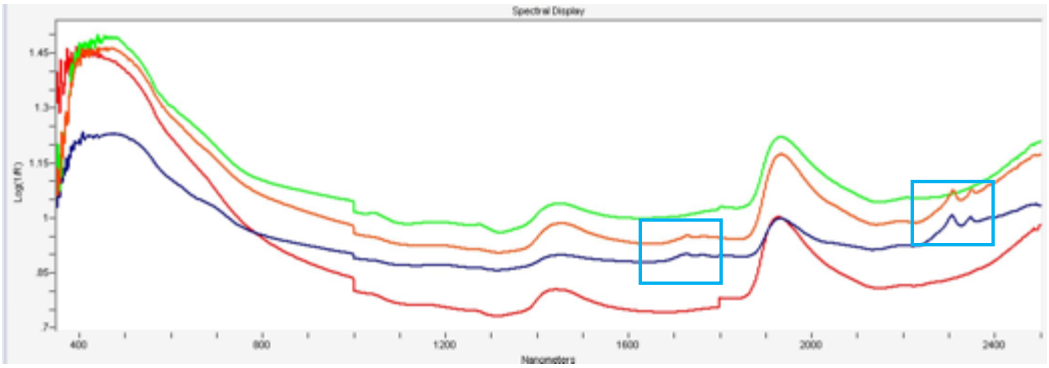

Figure 4.13: Soil spectra with decomposition peaks present. Decomposition peaks are highlighted by blue boxes. The red and green spectra without a blue box indicate spectra have not been impacted by decomposition fluid and do not display these peaks in their output.

Results for Cross-Sectional Sample Set for Research Question 3

To address whether the spectral signature of human decomposition fluid is detectable in plant leaves overtime after the cessation of active decomposition the cross-sectional sample set was used.

Plant Leaves

To address whether the spectral signature of human decomposition fluid is detectable in plant leaves after the cessation of active decomposition, the cross-sectional sample set was analyzed. For all cross-sectional plant samples, the bands that primarily account for the variation in PC1, are 2170-2174 nm. The bands that account for the variation in PC2 are 2040-2042 nm. The bands from both PC1 and PC2 are associated with proteins. All decomposition fluid was compared to the plant leaf samples in the cross-sectional PCA. Each result shows that PC1 primarily accounts for the variation in the spectra of the plant samples, while PC2 displays the variation in decomposition fluid (Figures 4.14). Plants are closely grouped together with the exception of the leaves from Plants 9.2, 12.1, 12.2, 13.1, and 13.2. None of these plants' leaves grouped with decomposition fluid. The difference in groupings of the plant leaves from Plants 9.2, 12.1, 12.2, 13.1, and 13.2. is likely due to variation between the individual plant leaves, not due to the presence of cadaveric materials at the selected bands for analysis. Variation in the plant could be attributed to the age of the plant, the area of the ARF the plant was located in, or the overall health of the plant. The lack of grouping between any decomposition fluid and plants indicates that cadaveric material from the selected bands

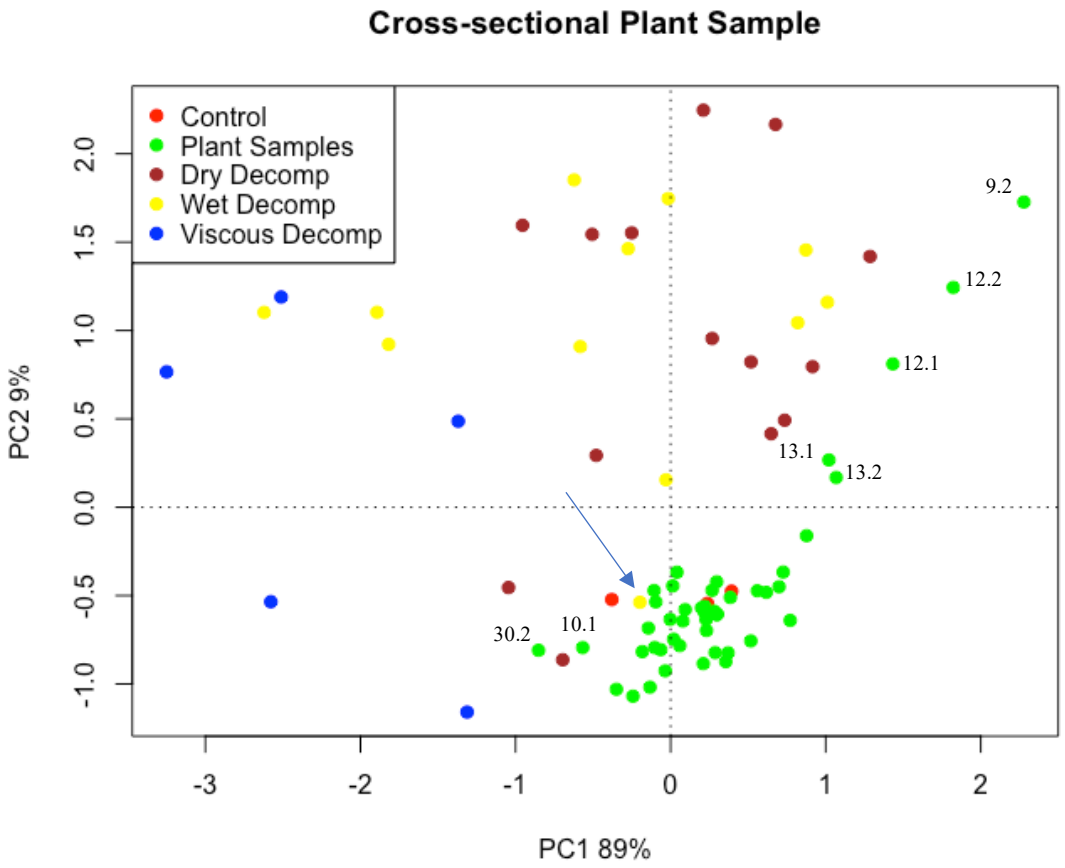

Figure 4.14: PCA for all decomposition fluid and the leaves of the cross-sectional plant dataset. The bands that account for the variation among the samples in PC1 are 2170-2174 nm. The bands that account for the variation among the samples in PC2 are 2040-2042 nm. These bands are associated with proteins. Note the grouping of most plants including the control plants centered around the axes of PC1 and 2. The leaves of plants 9.2, 12.1, 12.2, 13.1, and 13.2 do not group with the other plant leaves. However, they also do not group with decomposition indicating that the variation is among plant differences, not due to lipids, proteins, or carbohydrates present in the spectra. Plants 10.1 and 30.2 do group with decomposition fluid; however, this grouping is likely not due to the concentration of lipids, carbohydrates, and protein in the plant spectra. Rather it is likely due to organic leaf material being sampled in the decomposition fluid. The blue arrow is pointing to a wet decomposition fluid spectra that groups both control and test plant samples. This is also likely due organic leaf material in the decomposition sample.

is not detectable in the plant leaves after active decomposition ceases.

Plants 10.1 and 30.2 do group with dry decomposition fluid; however, this grouping is likely not due to the concentration of lipids, carbohydrates, and protein in the plant spectra. Rather the grouping is likely due to organic leaf material being sampled in the decomposition fluid (Figure 4.14). A wet decomposition fluid sample is also grouped with plants, including a control. The grouping of this wet decomposition sample is also likely also due organic leaf material in the sample. The presence of organic leaf material in the samples is a result of sampling the decomposition spectra directly on the ground.

Soil

For all cross-sectional soil samples, the bands that primarily account for the variation in PC1 are 2170-2174 nm, reflective of proteins. The bands that account for the variation in PC2 are 1690-1694 nm, reflective of carbohydrates. All decomposition fluid was compared to the soil samples in the cross-sectional PCA. Each result shows that PC1 primarily accounts for the variation in the soil samples, while PC2 displays the variation in decomposition fluid (Figure 4.15). Some soil samples are closely grouped with all three types of decomposition fluid, such as those from Donors 3, 16, 18, 23, 24, 28, 29, and 30. These groupings indicate that the soil spectra from these donors have high enough concentrations of cadaveric materials at the selected bands to be detected spectrally even after the cessation of active decomposition. The soil sampled that did not group with decomposition do not have high enough levels of cadaveric materials to be detected spectrally after the cessation of active decomposition.

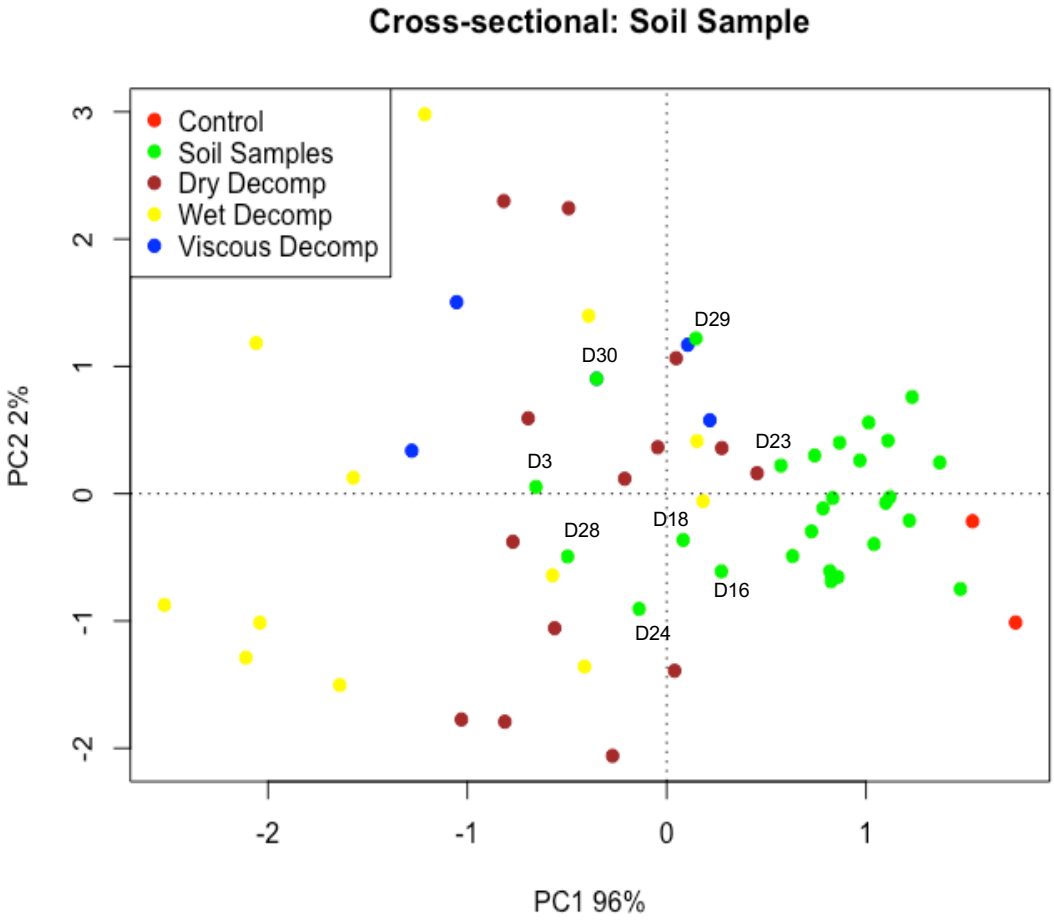

Figure 4.15: PCA for all decomposition fluid and cross-sectional soil sample set. Note that Donors 3, 16, 18, 23, 24, 28, 29, and 30 group within viscous, wet, and dry decomposition, while the other soil spectra including the controls are group together. The eight samples that group with decomposition fluid have spectral concentrations of lipids, carbohydrates, and proteins that are similar to decomposition fluid. The bands that account for the variation among the samples in PC1 are 2170-2174 nm, reflective of proteins. The bands that account for the variation in PC2 are 1690-1694 nm, reflective of carbohydrates.

CHAPTER FIVE

DISCUSSION AND CONCLUSIONS

This study assessed the applicability of using FORS to identify a detectable decomposition fluid spectrum and determine whether that spectrum can be identified in both plants and soil located in the direct vicinity of a body. There were three research questions asked in this study:

1. Does human decomposition fluid have a detectable spectral signature that can be found in fluids shed from the body in an outdoor environment?
2. Can the spectral signature of human decomposition fluid be detected in both plant leaves and soil during active decomposition?
3. Does the spectral signature of human decomposition fluid persist in the plant leaves and soil after the cessation of active decomposition?

The results reveal new information regarding the spectral signature of human decomposition, and the applicability and ability to identify this signature using remote sensing spectroscopy.

The Spectral Signature of Human Decomposition

The peaks reflective of lipids, carbohydrates, and proteins the NIR and SWIR regions of the EMS demonstrate that human decomposition fluid exhibits a spectral signature. Results of the PCA statistical analysis of the decomposition fluid signature shows that the decomposition fluid varies from other material (plant leaves and soil). Carbohydrates and lipids, found in bands, 1690-1694 nm and 2352-2354 nm respectively

account for the highest concentration of decomposition fluid. Both soil and plants have different bands that account for the most variance in their samples, which will be discussed later in this chapter.

Overall, decomposition fluid signatures do not group by or between fluid type (viscous, wet, or dry) and their results are dispersed through the PCA (Figure 4.5). Differences in the type of the decomposition fluid, the chemical make-up, and concentrations of cadaveric materials within the fluid itself could be a factor in the difference between types. By taking the spectral samples of decomposition fluid directly on the ground, both dry and wet decomposition have the potential to have interference from other organic material, such as soil and leaf litter. Viscous decomposition typically has a thick enough consistency that the contact probe does not touch the ground so there is less of a potential to come into contact with other organic material compared to wet or dry decomposition (Figure 3.7).

The Presence of Decomposition Fluid in Plant Leaves and Soil Spectra

The results from research questions 2 and 3 are similar and indicate that human decomposition is not detectable within the NIR and SWIR region of the EMS in plant leaf samples but is detectable in some soil spectra. Based on the 62 bands selected, the results do not show the presence of decomposition fluid in plant leaves being impacted by active decomposition fluid, or that plants were impacted by decomposition fluid. The results show that based on the 62 bands selected plant leaf spectra do not group with decomposition fluid, indicating that the spectra do not contain either lipids,

carbohydrates, or proteins. However, the bands that provide the most concentration in the spectral samples of the plant leaves are 2170-2174 nm and 2040-2043 nm, which account for proteins. The concentration of these bands in the plant samples were not close enough to the decomposition characteristics to be grouped together. The presence of proteins could be indicative of the protein levels naturally found in plants.

In some soil samples, statistical results indicate that decomposition fluid is detectable in soil and decomposition fluid characteristics can be identified in soil spectra. Soil samples directly associated with human decomposition can be identified based on their proximity to decomposition samples within the PCA analysis; the samples group closely with one another. There is no difference between the type of decomposition fluid that groups with soil spectra, and all three types of decomposition fluid groups with soil. Similarly, to plants, the bands that primarily account for the concentration in the soil spectra are 2040-2045 nm and 2170-2174 nm and are indicative of proteins. Decomposition characteristics are detectable in soil samples both during active decomposition and after active decomposition has stopped. However, decomposition fluid characteristics are not detectable in all samples. For example, Donor 31 did not have any soil spectral samples that grouped with decomposition fluid, while Donor 37 had multiple samples that grouped decomposition fluid. The difference between donors could be related to the amount of decomposition fluid released from the donor and taking the sample directly on the group surface. When collecting the soil spectra directly on the ground surface during active decomposition, where decomposition fluid was released,

there is the potential to be sampling more fluid than soil and this could have been the case for some samples from Donor 37, especially those in blocks D3, 4 (Figure 3.9).

For the cross-sectional dataset only the soil spectra from 8 out of 27 donors grouped with decomposition fluid. The donors that grouped with decomposition were placed in either 2019, 2020, or 2021. Donors placed before 2019 do not appear to group with decomposition fluid. This indicates that time since placement may influence concentrations of detectable levels. Environmental conditions such as the amount of rain the soil is exposed to or the amount of sun versus shade the soil is exposed to may influence the concentrations of decomposition fluid present for detection. A larger sample size is needed to determine whether time since placement or other environmental variables affect the presence of detectable spectral signatures of cadaveric materials *via* FORS. The decreased concentration of cadaveric materials in soils placed before 2019 could be due to weather or soil erosion. The amount of fluid released during active decomposition may not have been enough to remain prominent in the soil or microbes present in the soil consumed portions of the decomposition fluid.

The different consistency of decomposition fluid, the amount of decomposition fluid, and the soil type can all play an important role in the appearance of spectral characteristics. When taking the spectra of soil directly on the ground where an individual decomposed there is the potential to be sampling more dry decomposition rather than soil. Another factor that should be considered is that the ARF has been used for almost 40 years and the ground has been continuously saturated by decomposition fluid. This

continuous saturation with decomposition fluid could bias the results for some samples by having higher concentration of lipids, carbohydrates, and protein present than soil not previously impacted by decomposition fluid. Despite this deep history of use at ARF, plants are not taking up lipids, carbohydrates, and proteins in high enough concentrations to be detected spectrally. The plant spectra are similar to the control samples taken both inside and outside of the ARF. The plants could not be taking up the cadaveric materials because of the changes to the pH in the soil. As previously discussed, the decomposition fluid reduces the pH of soil causing it to become acidic. Plants growing in acidic soil cannot readily intake and metabolize nutrients through their root systems.

Conclusions

Locating missing deceased individuals can pose a significant challenge to law enforcement. This study aims to take the first step in evaluating the efficacy of using remote sensing technology, specifically FORS, to evaluate whether or not remote sensing through FORS is an applicable method to identify decomposition fluid in the environment. The research is valuable as it shows that decomposition fluid does have a detectable spectral signature visible in the NIR and SWIR regions of the EMS. The signature shows peaks in regions where lipids, carbohydrates, and proteins are found. When looking at the selected bands in the NIR regions, the leaves of Amur honeysuckle do not appear to display any detectable decomposition fluid characteristics. However, there are visible peaks in the selected regions of the soil spectra once it has been impacted by decomposition fluid. Qualitatively, there are visible differences in decomposition fluid

spectra from that of plant leaves and soil. These differences can be seen in the soil spectra impacted by decomposition fluid versus soil spectra that has not been impacted (Figure 4.13). However, quantitively, in the PCA analysis, there does not seem to be major changes between decomposition fluid, plant leaves, or soil either during active decomposition or advanced decomposition. There are many factors that can affect the presence of cadaveric materials visible in the spectra. How plants can metabolize the by-products of decomposition fluid in acidic soil may affect its visibility in spectra. For soil however, decomposition fluid is released directly onto the soil surface. It only seeps into the soil about 3cm below the surface, leaving much of the fluid to remain on the surface where the samples were collected (Cobaugh et al. 2015).

There are limitations to the study that should be addressed. First, only one plant species was analyzed. Other plant species may be affected differently by decomposition fluid by-products and display different spectral peaks than Amur honeysuckle. Second, only the decomposition fluid of humans was analyzed. The signature of decomposition fluid from other animals may have a similar signature, which can complicate searching for a deceased individual in natural areas where other animals may have also decomposed on the ground surface. Additional research should be done to compare the decomposition signature of animals to humans to identify any similarities or differences. There may also be differences in the signature of decomposition fluid between humans based on their individual chemical compositions and intrinsic variables (Mason et al. 2022). Comparing the decomposition fluid between individual is also an area of future research that should

be addressed. A further limitation is that the donors, plants, and soil in this study are bounded by the specific environmental conditions of ARF and the decomposition process in East Tennessee. Specifically, the facility's continued use has likely altered the soil chemistry (Damann et al 2012). Therefore, the results of this study are not directly comparable soil not previously impacted by decomposition. While one goal of this research is to use an instrument that can be easily portable in the field, many environmental factors that cannot be controlled when collecting data in the field. For example, other organic material, such as leaf litter in the decomposition fluid spectra, particularly in dry decomposition, may affect the spectral reflectance intensity (Figure 4.14).

Only certain wavelength bands were selected for study based on previous research that looked at animal fats, urine, and eggs in paint (Horn 2018). The results from Horn's work were used as a proxy for human decomposition fluid. Additional research should be done to analyze additional bands that may provide more information on plant health and nitrogen leaves the presence of decomposition in plant spectra by looking at the bands around 600-800 nm may provide additional information (Capelle and Macko 2016; Gupta 2017). While the decomposition signature may not be present in the NIR and SWIR regions for plants, there may be changes to the overall plant health visible in other wavelength bands (Corcoran 2016). Additionally, analyzing the presence of nitrogen in plant leaves and soil as a results of decomposition fluid may be visible in the spectra. A more extensive longitudinal study analyzing the spectra of plants that have undergone

multiple growing seasons may yield difference in nutrients or nitrogen levels in their spectra.

Further research to investigate whether the height of the leaves sampled results in different spectral signatures is essential. For example, leaves near the ground are often killed by decomposition fluid, while those leaves higher on the plant remain healthy. Sampling leaves systematically at different heights may provide helpful information in interpreting changes to plant spectra that have been impacted by decomposition fluid. Additional research should investigate why the soil spectra for some donors have a detectable decomposition signature, while other donors did not. The research should address whether difference in detecting a spectral signature of decomposition between humans is due to body composition and intrinsic factors.

The search for missing deceased individuals is a difficult and time sensitive task. This study was designed to test whether FORS can be used to identify a detectable spectral signature of decomposition in plants and soil during active decomposition. FORS can identify a spectral signature of human decomposition. The decomposition signature is present in soil that has been impacted by decomposition. However, FORS cannot identify any spectral differences of the selected wavelength bands in Amur honeysuckle. Ultimately, FORS shows potential for locating missing deceased individuals from soil spectra even after the cessation of active decomposition This is useful in cases where the remains have been moved from the original decomposition site either from taphonomic

processes or human intervention. However, more research should be done to address the limitations of this study.

REFERENCES

Aggarwal, Shefali (2004) “Principles of Remote Sensing.” *Satellite Remote Sensing and GIS Applications in Agricultural Meteorology*. World Meteorological Organisation.

Aitkenhead-Peterson, J. A., C. G. Owings, M. B. Alexander, N. Larison, and J. A. Bytheway. (2012) "Mapping the lateral extent of human cadaver decomposition with soil chemistry." *Forensic science international* 216, no. 1-3: 127-134.

Aitkenhead-Peterson, Jacqueline A., James P. Fancher, Michael B. Alexander, Michelle D. Hamilton, Joan A. Bytheway, and Daniel J. Wescott. (2021) "Estimating postmortem interval for human cadavers in a sub-tropical climate using UV-Vis-near-infrared Spectroscopy." *Journal of Forensic Sciences* 66, no. 1:190-201.

Alam, Syed Manzoor., Naqvi, Syed Shamshad Mehdi Naqvi, & Ansari, Raziuddin (1999). Impact of soil pH on nutrient uptake by crop plants. *Handbook of plant and crop stress*, *2*, 51-60.

ASD Doucument 600545 Rev. E. (2008) RS^3 User Manual.

Barton, P. S., Reboldi, A., Dawson, B. M., Ueland, M., Strong, C., & Wallman, J. F. (2020). Soil chemical markers distinguishing human and pig decomposition islands: a preliminary study. *Forensic Science, Medicine and Pathology*, *16*(4), 605-612.

Bates, Lennon N., and Daniel J. Wescott. (2006) "Comparison of decomposition rates between autopsied and non-autopsied human remains." *Forensic science international* 261: 93-100.

Beattie, J. R., & Esmonde-White, F. W. (2021). Exploration of principal component analysis: deriving principal component analysis visually using spectra. *Applied Spectroscopy*, *75*(4), 361-375.

Bow, Sierra (2020). *Characterizing Late Pre-Contact Mississippian Paint Recipes in the Southeastern United States.* University of Tennessee, Knoxville Dissertation

Brabazon, Holly, Jennifer M. DeBruyn, Scott C. Lenaghan, Fei Li, Amy Z. Mundorff, Dawnie W. Steadman, and C. Neal Stewart. (2020) "Plants to Remotely Detect Human Decomposition?" *Trends in plant science* 25, no. 10:947-949.

Brown, David J., Keith D. Shepherd, Markus G. Walsh, M. Dewayne Mays, and Thomas G. Reinsch. (2006) "Global soil characterization with VNIR diffuse reflectance spectroscopy." *Geoderma* 132, no. 3-4: 273-290.

Butters, Owyn, Matt N. Krosch, Michell Roberts, and Donna MacGregor. (2021) "Application of forward-looking infrared (FLIR) imaging from an unmanned aerial platform in the search for decomposing remains." *Journal of Forensic Sciences* 66, no. 1: 347-355.

Campbell, James and Wynne, Randolph (2011). *Introduction to remote sensing* (5th ed.). Guilford Press

Capelle, Sonja K., and Stephen A. Macko. (2016) "Finding the Spectral Signature of 15 Nitrogen Isotopes in Plants by Hyperspectral Techniques." *Journal of Remote Sensing* 4, no. 1: 115-120.

Carter, David, David Yellowlees, and Mark Tibbett. (2007). "Cadaver Decomposition in Terrestrial Ecosystems." *Naturwissenschaften* 94 (1): 12-24.

Cobaugh, and DeBruyn, J. M. (2013). *Soil microbial community succession during cadaver decomposition*. The University of Tennessee, Knoxville.

Cobaugh, Kelly L., Sean M. Schaeffer, and Jennifer M. DeBruyn. (2015) "Functional and structural succession of soil microbial communities below decomposing human cadavers." *PloS one* 10, no. 6: e0130201.

Corcoran, Katie Ann. (2016). A characterization of human burial signatures using spectroscopy and LIDAR. University of Tennessee, Knoxville Dissertation

Corcoran, Katie A., Amy Z. Mundorff, Devin A. White, and Whitney L. Emch. (2018) "A novel application of terrestrial LIDAR to characterize elevation change at human grave surfaces in support of narrowing down possible unmarked grave locations." *Forensic science international* 289:320-328.

Cramer, Grant R., Kaoru Urano, Serge Delrot, Mario Pezzotti, and Kazuo Shinozaki. "Effects of abiotic stress on plants: a systems biology perspective." (2011). *BMC plant biology* 11, no. 1: 1-14.

Danner, M., M. Locherer, T. Hank, and K. Richter (2015). "Spectral Sampling with the ASD FieldSpec 4 – Theory, Measurement, Problems, Interpretation." *EnMAP Field Guides Technical report*: GFZ Data Services.

Damann, Franklin E., Aphantree Tanittaisong, and David O. Carter. (2012) "Potential carcass enrichment of the University of Tennessee Anthropology Research Facility: a baseline survey of edaphic features." *Forensic Science International* 222, no. 1-3: 4-10.

Dunn, B. W., G. D. Batten, H. Geoffrey Beecher, and Susan Ciavarella. "The potential of near-infrared reflectance spectroscopy for soil analysis—a case study from the Riverine Plain of south-eastern Australia." *Australian Journal of Experimental Agriculture* 42, no. 5 (2002): 607-614.

Fahey, Catherine, and Stephen Luke Flory. (2022) "Soil microbes alter competition between native and invasive plants." *Journal of Ecology* 110, no. 2:404-414.

Forbes, S. L., Perrault, K. A. and Comstock, J. L. (2017). Microscopic Post-Mortem Changes: the Chemistry of Decomposition. In Taphonomy of Human Remains: Forensic Analysis of the Dead and the Depositional Environment (eds E. M. Schotsmans, N. Márquez-Grant and S. L. Forbes

Galloway, A., Birkby, W. H., Jones, A. M., Henry, T. E., & Parks, B. O. (1989). Decay Rates of Human Remains in an Arid Environment. *Journal of Forensic Sciences*, 34(3), 607-616.

Gull, Audil, Ajaz Ahmad Lone, and Noor Ul Islam Wani. (2019) "Biotic and abiotic stresses in plants." *Abiotic and biotic stress in plants*: 1-19.

Gupta, Ravi P. (2018) *Remote Sensing Geology*. 3rd ed. Berlin, Heidelberg: Springer Berlin Heidelberg.

Gürtler, Salete, Carlos R. Souza Filho, Ieda D. Sanches, Lucíola A. Magalhães, Marcos N. Alves, Wilson J. Oliveira, and Giuliana CM Quitério. (2022) "Leaf Spectra Changes of Plants Grown in Soils Pre-and Post-Contaminated with Petroleum Hydrocarbons." *Remote Sensing* 14, no. 14:3475.

Horn, Karen R. (2018) "Time Takes Its Toll: Detection of Organic Binder Media in Ochre Paints with Visible Near-Infrared and Short-Wave Infrared Reflectance Spectroscopy." *Journal of archaeological science reports* 21: 10–20

Hyde, Embriette R., Jessica L. Metcalf, Sibyl R. Bucheli, Aaron M. Lynne, and Rob Knight. (2017) "Microbial communities associated with decomposing corpses." *Forensic microbiology* 245.

Huete, Alfredo R., Ray D. Jackson, and D. F. Post. (1985) "Spectral response of a plant canopy with different soil backgrounds." *Remote sensing of environment* 17.1

Jackson, Ray D. (1986) "Remote sensing of biotic and abiotic plant stress." *Annual review of Phytopathology* 24, no. 1: 265-287.

Janaway, Robert C., Steven L. Percival, and Andrew S. Wilson. (2009) "Decomposition of human remains." *Microbiology and aging: clinical manifestations*.

Jansen, Marcel AK, and Geert Potters. (2017) "Stress: The way of life." *Plant stress physiology* (2017): ix-xiv.

Jones H. G. and P. Schofield (2008) "Thermal and Other Remote Sensing of Plant Stress." Gen. Appl. Plant Physiology, Special Issue 34 *(1-2), 19-3*

Karamanos, R. E. (2013). Nutrient uptake and metabolism in crops. *Prairie Soils and Crops*, *6*, 52-63.

Kim, Hyun Uk. "Lipid metabolism in plants." (2020) *Plants* 9, no. 7: 871.
Liu, Jinbao, Jichang Han, Yang Zhang, Huanyuan Wang, Hui Kong, and Lei Shi. (2018) "Prediction of soil organic carbon with different parent materials development using visible-near infrared spectroscopy." *Spectrochimica Acta Part A: Molecular and Biomolecular Spectroscopy* 204: 33-39.

Mandoli, D. F., Ford, G. A., Waldron, L. J., Nemson, J. A., & Briggs, W. R. (1990). Some spectral properties of several soil types: implications for photomorphogenesis. *Plant, Cell & Environment*, *13*(3), 287-294.

Marks, Murray, Love, Jennifer, and Dadour IR. (2009). Taphonomy and Time: Estimating the Postmortem Interval. In: Steadman DW, editor. Hard Evidence: Case Studies in Forensic Anthropology. New York: Taylor and Francis.

Mason, Allison R., Hayden S. McKee-Zech, Katharina M. Hoeland, Mary C. Davis, Shawn R. Campagna, Dawnie W. Steadman, and Jennifer M. DeBruyn. (2022) "Body mass index (BMI) impacts soil chemical and microbial response to human decomposition." *Msphere* 7, no. 5:e00325-22.

Megyesi, Mary, Nawrocki, Stephen, and Haskell, Neal (2005). "Using accumulated degree-days to estimate the postmortem interval from decomposed human remains." Journal of Forensic Sciences 50(3): 618-626.

Milton, Edward J., Michael E. Schaepman, Karen Anderson, Mathias Kneubühler, and Nigel Fox. (2009) "Progress in field spectroscopy." *Remote Sensing of Environment* 113: S92-S109.

Muñoz-Huerta, Rafael F., Ramon G. Guevara-Gonzalez, Luis M. Contreras-Medina, Irineo Torres-Pacheco, Juan Prado-Olivarez, and Rosalia V. Ocampo-Velazquez. (2013)

"A review of methods for sensing the nitrogen status in plants: advantages, disadvantages and recent advances." *sensors* 13, no. 8: 10823-10843.

Nduwamungu, Ziadi, N., Parent, L.-E., Tremblay, G. F., & Thuries, L. (2009). Opportunities for, and limitations of, near infrared reflectance spectroscopy applications in soil analysis: A review. *Canadian Journal of Soil Science*, *89*(5), 531–541.

Reeves, James (2010). Near- versus mid-infrared diffuse reflectance spectroscopy for soil analysis emphasizing carbon and laboratory versus on-site analysis: Where are we and what needs to be done? *Geoderma*, *158*(1), 3–14.

Roberts, Lindsey G., Jessica R. Spencer, and Gretchen R. Dabbs. (2017) "The effect of body mass on outdoor adult human decomposition." *Journal of forensic sciences* 62, no. 5:1145-1150.

Schwartz, Guy, Gil Eshel, and Eyal Ben Dor. (2011). "Reflectance spectroscopy as a tool for monitoring contaminated soils." *Soil Contamination.*

Summers, David, M. Lewis, Bertram Ostendorf, and David Chittleborough. (2011). "Visible near-infrared reflectance spectroscopy as a predictive indicator of soil properties." *Ecological Indicators* 11, no. 1: 123-131.

Schweiger, Anna K. (2020) "Spectral field campaigns: planning and data collection." *Remote sensing of plant biodiversity*: 385-423.

Sun, Wang, X., Wang, Z., Yang, L., Xie, Y., Huang, Y. (2021). UAVs as remote sensing platforms in plant ecology: review of applications and challenges. *Journal of Plant Ecology*, *14*(6), 1003–1023.

Taylor, Lois S., Adrian Gonzalez, Michael E. Essington, Scott C. Lenaghan, C. Neal Stewart, Amy Z. Mundorff, Dawnie W. Steadman, and Jennifer M. DeBruyn. (2023) "Soil elemental changes during human decomposition." *Plos one* 18, no. 6

Thermoscientific Grams IQ User Manal v.9.1 (2012), “Chemometrics Training Manual for Grams IQ/IQ Predict v9.1.

Tibbett, Mark and David O. Carter (2008) *Soil Analysis in Forensic Taphonomy: Chemical and Biological Effects of Buried Human Remains*. Boca Raton: CRC Press, 2008. Print.

Trouvelot S, Héloir MC, Poinssot B, Gauthier A, Paris F, Guillier C, Combier M, Trdá L, Daire X, Adrian M. (2014) Carbohydrates in plant immunity and plant protection: roles and potential application as foliar sprays. Front Plant Sci.

van der Merwe, Burchfield, D. R., Witt, T. D., Price, K. P., & Sharda, A. (2020). Drones in agriculture. In *Advances in Agronomy* (Vol. 162, pp. 1–30).

van der Straeten, Chaerle, Laury, and Dominique (2000) “Imaging Techniques and the Early Detection of Plant Stress.” *Trends in plant science* 5.11: 495–501.

Weidenhamer, Jeffrey D., and Ragan M. Callaway. (2010) "Direct and indirect effects of invasive plants on soil chemistry and ecosystem function." *Journal of chemical ecology* 36: 59-69.

APPENDIX 1

Table A.1 Donor Demographics

Donor Numbering	Placement Date	Sex: Female (F) Male (M)	Age	Sample Set: Cross-sectional (C) Longitudinal (L)
1	11-Jan-20	F	85	C
2	6-May-19	F	60	C
3	16-Apr-21	M	68	C
4	15-Apr-19	M	54	C
5	18-Sep-20	M	89	C
6	26-Apr-19	F	71	C
7	15-Jul-21	F	48	C
8	13-Jul-21	F	59	C
9	18-Mar-22	M	91	C
10	8-Jan-20	M	82	C
11	6-Jan-20	M	64	C
12	17-Nov-21	M	49	C
13	15-Apr-21	M	72	C
14	12-Jul-18	M	87	C
16	18-Sep-20	M	66	C
17	7-May-18	M	60	C
18	18-Sep-19	F	56	C
19	1-Feb-22	M	74	C
20	11-Oct-21	F	73	C
21	12-Nov-21	F	69	C
22	1-Jul-21	F	26	C
23	17-Sep-20	M	74	C
24	6-Aug-21	M	65	C
27	29-Apr-17	M	79	C
28	5-Nov-21	F	74	C
29	5-Nov-21	F	78	C
30	15-Jun-21	F	71	C
31	9-Apr-21	M	62	L-Trial 1 Plot 2- Soil only
33	28-Jun-21	F	65	L-Trial 2 Plot 2- Plants and Decomposition
34	28-Jun-21	M	67	L-Trial 2- Plot 3 Plants and Decomposition
36	7-Sep-21	M	88	L-Trial 3- Plot 2 Plants and Decomposition
37	7-Sep-21	F	86	L-Trial 3 Plot 3- Soil, Plants, and Decomposition

Table A.2: Date and Types of Decomposition Fluid Sampled Longitudinal Donors

Donor Number	Sample Date	Decomposition Fluid Type*
33	6-Jul-21	VD
33	8-Jul-21	WD
33	21-Jul-21	WD
33	2-Aug-21	DD
33	12-Oct-21	DD
33	11-Nov-21	DD
33	29-Nov-21	DD
34	13-Jul-21	VD
34	21-Jul-21	WD
34	26-Jul-21	WD
34	4-Aug-21	WD
34	9-Aug-21	DD
34	12-Oct-21	DD
34	26-Oct-26	DD
34	11-Nov-21	DD
34	29-Nov-21	DD
36	14-Sep-21	VD
36	23-Sep-21	VD
36	30-Sep-21	WD
36	12-Oct-21	WD
36	20-Oct-21	WD
36	26-Oct-21	WD
36	1-Nov-21	WD
36	9-Nov-21	DD
36	29-Nov-21	DD
37	16-Sep-21	VD
37	26-Oct-21	WD
37	1-Nov-21	WD
37	8-Nov-21	DD
37	16-Nov-21	DD
37	28-Nov-21	DD

*VD indicates viscous decomposition fluid, WD indicates wet decomposition fluid, and DD indicates dry decomposition fluid.

Table A.3 List of Average Number of Decomposition Spectral Samples per Collection Analyzed per Plot.

Trial 2 Plot 2 Donor 33
24
Trial 2 Plot 3 Donor 34
23
Trial 3 Plot 2 Donor 36
23
Trial 3 Plot 3 Donor 37
24

Table A.4: Sampling Dates of Plants for Each Trial for Longitudinal Plant Leaves Sample Set

Trial 2 Sampling Dates	Trial 3 Sampling Dates
28-Jun-21	7-Sept-21
6-Jul-21	14-Sep-21
9-Jul-21	23-Sep-21
13-Jul-21	30-Sep-21
16-Jul-21	12-Oct-21
19-Jul-21	20-Oct-21
26-Jul-21	26-Oct-21
2-Aug-21	1-Nov-21
9-Aug-21	8-Nov-21
20-Aug-21	29-Nov-21
27-Aug-21	16-Jun-22
2-Sep-21	17-Jun-22
16-Sep-21	
28-Sep-21	
12-Oct-21	
26-Oct-21	
11-Nov-21	
29-Nov-21	
16-Jun-22	
17-Jun-22	

Table A.5 List of Average Number of Spectral Samples per Collection Analyzed per Plant.

Trial 2 Plot 2 Donor 33	**Average Spectral Samples/Plant**
Plant 1	71
Trial 2 Plot 3 Donor 34	**Average Spectral Samples/Plant**
Plant 2	70
Trial 3 Plot 2 Donor 36	**Average Spectral Samples/Plant**
Plant 3	67
Trial 3 Plot 3 Donor 37	**Average Spectral Samples/Plant**
Plant 1	69
Plant 2	70

Table A.6: Sampling Dates of Soil for Donors 31 and 37

Donor 31	Donor 37
9-Apr-21	7-Sep-21
12-Apr-21	16-Sep-21
16-Apr-21	28-Sep-21
19-Apr-21	12-Oct-21
23-Apr-21	19-Oct-21
26-Apr-21	1-Nov-21
7-May-21	16-Nov-21
14-May-21	
21-May-21	
30-Jun-21	
9-Aug-21	
30-Nov-21	

Table A.7. Donor Placement Date, Plant I.D, Location to Donor, and Distance from Donor Groin

Donor Number	Placement Date	Plant ID	Uphill (U)/Downhill (D)/ Even Slope (E)	Distance from Donor Groin
1	11-Jan-20	1.1	U	140cm
		1.2	D	130cm
2	6-May-19	2.1	U	100cm
3	16-Apr-21	3.1	E	210cm
		3.2	E	120cm
4	15-Apr-19	4.1	U	100cm
		4.2	D	140cm
5	18-Sep-20	5.1	U	180cm
		5.2	D	130cm
6	26-Apr-19	6.1	U	250cm
		6.2	D	130cm
7	15-Jul-21	7.1	U	200cm
		7.2	D	80cm
8	13-Jul-21	8.1	U	150cm
		8.2	D	100cm
9	18-Mar-22	9.2	D	150cm
		9.3	D	200cm
10	8-Jan-20	10.1	U	210cm
		10.2	D	230cm
11	6-Jan-20	11.2	D	220cm
12	17-Nov-21	12.1	U	250cm
		12.2	D	290cm
13	15-Apr-21	13.1	U	160cm
		13.2	D	80cm
14	12-Jul-18	14.1	U	90cm
		14.2	D	150cm
16	18-Sep-20	16.1	U	140cm
		16.2	D	160cm
17	7-May-18	17.2	D	160cm

Table A.7. Continued:

Donor Number	Placement Date	Plant ID	Uphill (U)/Downhill (D)/ Even Slope (E)	Distance from Donor Groin
18	18-Sep-19	18.1	U	100cm
		18.2	D	160cm
19	1-Feb-22	19.1	D	110cm
		19.2	U	190cm
20	11-Oct-21	20.1	U	220cm
		20.2	D	100cm
21	12-Nov-21	21.1	U	190cm
		21.2	D	50cm
22	1-Jul-21	22.1	U	230cm
		22.2	D	130cm
23	17-Sep-20	23.1	D	120cm
		23.2	U	200cm
24	6-Aug-21	24.1	U	200cm
27	29-Apr-17	27.1	D	160cm
28	5-Nov-21	28.1	D	110cm
		28.2	U	120cm
29	5-Nov-21	29.1	D	170cm
		29.2	U	190cm
30	15-Jun-21	30.1	U	200cm
		30.2	D	200cm

Table A.8: Selected Wavelength Bands

Selected Wavelength Bands	
1690	2055
1691	2056
1692	2057
1693	2058
1694	2059
1724	2060
1725	2061
1726	2062
1727	2063
1761	2064
1762	2170
1763	2171
1764	2172
1825	2173
1826	2174
1827	2317
1828	2318
2040	2319
2041	2320
2042	2321
2043	2346
2044	2347
2045	2348
2046	2349
2047	2350
2048	2351
2049	2352
2050	2353
2051	2354
2052	
2053	
2054	

APPENDIX A

Operating Procedures for Collecting Data with the ASD FieldSpec 4:

Guide for Collection created by Dr. Sierra Bow.

Setting Up the Instrument:

Remove the instrument, computer, contact probe, battery, reflectance panel, and all associated connection cables from the case.

1. Place the laptop with the laptop carrier.

2. Place the instrument within the backpack carrier and secure with the five strap connectors. Place the fiber optic cable on the side of your nondominant hand.

3. Connect the instrument to power with the battery. The power cord is located on the right hip-pouch of the backpack carrier. Place battery cell in this pouch after attaching power cable to the instrument.

4. Connect the controller computer to the instrument using the Ethernet cable.

5. Connect the contact probe:
    a. Unscrew the strain relief fitting and remove the small plastic fiber optic adapter. Slide the strain relief fitting, coil end first, onto the fiber optic cable. Slide the small plastic adapter, wide end first, onto the fiber optic cable.
    b. Insert the tip of the fiber optic cable into the opening in the Contact Probe. Make sure it is fully inserted into the opening.
    c. While holding the fiber optic cable in place, slide the small plastic adapter into the Contact Probe fitting. Make sure it is fully seated. Connect the strain relief fitting and tighten by hand so that the fiber optic cable will not slide backwards.
    d. Verify the tip of the fiber optic cable is positioned fully forward and can be clearly seen through the window on the end of the Contact Probe. Adjust as needed.
    e. Connect the contact probe power cable to the instrument.

6. Turn on the instrument by pressing the button on the side of the instrument.

7. Turn on the contact probe light source by pressing the button on the probe.

8. Let the instrument and light source warm up for at least 15 minutes. In colder conditions increase warm up time to 30 minutes.

9. Put on backpack carrier first. Secure the chest and hip chips.

10. Put on the laptop carrier and adjust straps as necessary. There are also clips to secure carrier to the backpack carrier.

11. Turn on the computer and connect to RS³ software.

RS³ Set Up and Saving Spectra:

After you have set up the instrument for use and are ready to collect spectra, you must optimize and set a white reference.

1. Start the RS³ software. Icon is located on the desktop. If using one of the default network configurations, RS³ automatically detects and connects to the instrument.

2. Verify the Power Status, located at the bottom of the main window. The volt level of the spectrometer will be reported in the balloon type window.

3. Verify the Connection Status, located next to the Power Status. A balloon type window will indicate the connection status of the instrument.

4. Point the end of the fiber optic cable at the Spectralon reference panel. Keep it on the panel until the next steps are completed.

5. Click Opt (button located on the toolbar) to optimize the instrument. The the conditions and set-up of the reference panel should be identical to how the samples will be measured.
   - The optimization is complete when the Spectrum Avg progress bar resumes.

6. Click WR (button located on the toolbar) to take a white reference.
   - A white reference is only useful when collecting reflectance data. This step is not necessary when collecting radiance or irradiance data.
   - The white reference is complete when the Spectrum Avg progress bar resumes.
   - The white reference sample should be a straight line at the reflectance value 1

7. Select Control > Save Spectrum. Here you can change many things:
   - Path Name: the directory folder where files are to be saved. *Note: create a directory structure outside of C:\Program Files\RS3.
   - Base Name: When Save As New File Format is checked, the base name can be up to 27 characters long. The base name is concatenated with an

incrementing five-digit sample number followed by an .asd extension (i.e. DataCollection00001.asd). When Save As New File Format is unchecked the base name only allows 8 characters in the filename used in each data file. *Note: base names should relate to the samples being collected.
    - Starting Spectrum Num: This field is the starting point for the five-digit file extension given to the filename. You can only enter the starting value. Whenever a spectrum of sequence of spectra is saved, this number automatically increments.
    - Number of files to save: This field specifies how many total files are to be created each time the spectrum is saved. For example, if you choose 00003, then three individual files will be saved simultaneously for each spectrum you collect.

8. Once all desired information is input in the Spectrum Save window do one of the following to begin collecting data:
    - To save the settings in the Spectrum Save window but not save any spectra yet, click OK. Then use the laptop space bar to begin saving your collected data.
    - To begin saving spectra immediately, click Begin Save. This will close the window and immediately collect and save whatever the fiber optics are pointed at. To save data afterwards, use the laptop space bar.
    - When spectra are saved through either initial method the laptop will chime each time data is collected/saved. Volume was kept loud to hear the chime to ensure each spectra was collected.

Optimizing During Data Collection:

Optimization is the process of setting the instrument's electronics to optimally process the incoming signal. This means that the digitalization of the light signal is within a range of values that provide good signal-to-noise performance and does not allow the instrument to saturate at the current light levels.

- The instrument must be re-optimized if:
    - The light source changes.
    - The instrument is in the process of warming up and the response changes substantially.
        - The instrument is saturating.

Use the Spectralon white reference panel when optimizing and for taking a white reference measurement. Follow steps 2 through 4.

White reference samples were taken at 15-minute intervals to ensure the instrument was optimized.

Wavelength Verification:

Prior to the operation of the instrument each session, wavelength verification needs to be monitored to ensure wavelength accuracy and assure collection of good quality spectra. You will need the instrument, laptop, Contact Probe, Spectralon white reference panel, and the Mylar card.

Allow the instrument and Contact Probe light source to warm up for 15-30 minutes prior to testing; then follow the steps below:

1. Place the Contact Probe on a clean Spectralon panel. Collect a white reference by clicking on the Baseline button. Make sure that 'Optimize First' box is checked.
2. Place the Mylar card on top of the Spectralon white reference panel.
3. Place the Contact Probe on top of the Mylar card.
4. Take a scan and observe the spectrum on the screen.
5. Compare the position of the peak on the screen to that on the Mylar card.
6. Peaks are allowed a +/- 1 nm difference from the printed standard.
7. If the peaks on the screen match the standards printed on the Mylar card your wavelength verification has yielded a "pass" result and you can continue with research data collection. If the peaks do not match the wavelength calibration may need to be adjusted. Do not collect any more spectra and contact ASD Technical Support.

General Instrument Care

Instrument Inspection:

Once per week the condition of the fiber optics should be checked using the Fiber Check utility. If large steps are present in collected data, fiber optics should be checked immediately as large, persistent steps can indicate broken fibers.

- To check the fiber optic cable for broken fibers:
    a. Remove any fore optic accessories from the instrument's fiber optic cable.
    b. Attach the fiber inspection scope/magnifier to the end of the fiber optic cable.
    c. Exit any ASD software that may be running and communicating with the unit.
    d. Ensure the instrument is turned on

e. Start the Fiber Check software (Start menu > All Programs > ASD Programs > RS³ Tools > Fiber Check)
f. Verify the IP address for the instrument
g. Select the desired LEDs to turn on and click Check. *Note: it is easier to check one fiber at a time. The LEDs flash very brightly.
h. Look through the magnifier to see which fiber illuminate and count the number of fibers that light. Each region has 19 individual micron fibers.
i. Repeat g-h process for each fiber.

Battery:

- A fully charged battery can be expected to run for over 4 hours using a contact probe in ambient environments.

- Do not unplug the charger and leave the battery in the charger. Remove the battery first, or the battery will discharge through the charger.

- Recharge a fully discharged battery as soon as possible (within 24 hours). Uncharged batteries will be incapable of accepting charge if the period of time between charges is too long.
    - A partially discharged battery does not need charging immediately.
    - A fully discharged battery will take approximately 8 hours to fully charge.
    - Constant overcharging or undercharging will shorten battery life.

- *Note: the instrument will stop collecting spectra when the battery drains to about 10 volts, and the software displays a message that says it is unable to collect. The instrument and any attached accessories, however, will continue to draw current if the power if left on. Turn off the instrument and remove all accessories as soon as possible when the message displays.

Spectralon Reflectance Panel:

- Care should be taken to prevent contaminants such as finger oils from contacting the material's surface.

    - If the material is lightly soiled, it may be airbrushed with a jet of clean dry air. *Note: do not use any compressed gas with freon propellant as it will damage the Spectralon surface.

- For heavier soil, the reflectance panel can be cleaned by sanding under running water with a 220-240 grit waterproof sandpaper until the surface is totally hydrophobic (water beads and runs off immediately). Gently move the panel in a figure-eight motion on the sandpaper, using water to wash away the thin layer that is sanded off. Blow dry with clean air or allow material to air dry overnight.

Ventilation Requirements:

Ensure the instrument is correctly placed within the backpack carrier to allow proper ventilation. Insufficient ventilation can result in overheating of the instrument, corrupted data, and possible physical damage to the instrument.

- Do not cover the vents of the instrument. When the instrument is placed within the backpack carrier, these vents will be facing upwards.

- Keep objects and spills (including rain) from entering or falling into the instrument and power supplies.

VITA

Anielle Constance Duncan was born in Knoxville, Tennessee. Anielle began her undergraduate degree at Pellissippi State Community College in August 2013. She graduated with an Associates of Arts Degree in July 2015 and then transferred to the University of Tennessee, Knoxville (UTK) to complete her Bachelor of Arts degree in Anthropology. She graduated from UTK in May 2017 Summa Cum Laude. Anielle began her Master of Arts degree in August 2019 at UTK under Dr. Dawnie Steadman.